Bioorganic Chemistry 85 (2019) 541–557

Contents lists available at ScienceDirect

Bioorganic Chemistry

journal homepage: www.elsevier.com/locate/bioorg

# Pyrazoles containing thiophene, thienopyrimidine and thienotriazolopyrimidine as COX-2 selective inhibitors: Design, synthesis, *in vivo* anti-inflammatory activity, docking and *in silico* chemo-informatic studies

Mai S. El-Shoukrofy[a,*], Heba A. Abd El Razik[a], Omaima M. AboulWafa[a], Aida E. Bayad[b], Ibrahim M. El-Ashmawy[b,c]

[a] Department of Pharmaceutical Chemistry, Faculty of Pharmacy, Alexandria University, 21521 Alexandria, Egypt
[b] Pharmacology Department, Faculty of Veterinary Medicine, Alexandria University, Alexandria, Egypt
[c] Department of Veterinary Medicine, Faculty of Agricultural and Veterinary Medicine, Qassim University, P.O. Box 1482, Buraydah, Al-Qassim, Saudi Arabia

ARTICLE INFO

*Keywords:*
Thiophenes
Thienopyrimidines
Pyrazoles
COX-1/COX-2 selectivity index
Anti-inflammatory activity
Ulcerogenic activity
Docking study
ADME
PreADMET
Drug-likeness model score

ABSTRACT

New thiophene and annulated thiophene pyrazole hybrids were synthesized and screened for their *in vitro* COX-1/COX-2 enzymatic inhibition and *in vivo* anti-inflammatory activities. All compounds were more COX-2 selective inhibitors than COX-1 with compound **13** exhibiting the highest COX-2 selectivity index. Compounds **3, 6a**, **9** and **11** were the most promising in the acute anti-inflammatory assay while compounds **3**, **5, 6a, 6c, 9, 10, 11** and **13** exerted promising anti-inflammatory activity in the sub-acute anti-inflammatory assay. Compounds **3, 6a**, **6c**, **9**, **10** and **11** were evaluated for their $ED_{50}$ values and were more potent than diclofenac sodium while compounds **6a**, **6c** and **9** were of greater potency than celecoxib with compound **6a** being the most potent showing $ED_{50}$ = 0.033 mmol/kg. These compounds were non-toxic and proved to be gastrointestinal safe compared to indomethacin, diclofenac sodium and celecoxib. Docking studies into COX-2 active site (PDB code 3LN1) revealed that compounds **3, 6a, 6c, 9, 10, 11** and **13** had binding modes and energies comparable to that of celecoxib. Compounds **3, 9, 10** and **11** complied with Lipinski's RO5 while compounds **6a** and **6c** showed one violation whereas compound **13** deviated by 2 violations. Compounds **6a, 6c** and **13** showed 100% plasma protein binding (PPB) and showed no aqueous solubility while compounds **3, 10** and **11** demonstrated the best drug likeness model scores. Therefore, the thiophene analog **3** and the thienopyrimidine derivatives **10** and **11** are promising anti-inflammatory candidates that exert moderate selective COX-2 inhibition with acceptable physicochemical properties.

## 1. Introduction

Inflammation is the initial defense response of the body cells and tissues to various stimuli such as pathogens, infections, irritation, chemicals, mechanical or thermal injuries [1]. It is clinically manifested as pain, swelling, heat, redness and aches at the inflamed tissues [2]. These symptoms are due to the release of some inflammatory mediators including prostaglandins (PGs), thromboxanes (TXs) and leukotrienes (LTs) [3]. Inflammatory diseases are commonly treated with non-steroidal anti-inflammatory drugs (NSAIDs) [4]. They exert their effect *via* the inhibition of cyclooxygenases (COXs) which catalyze the metabolism of arachidonic acid (AA) into PGs and TXs preventing their formation [4,5]. COXs were discovered to exist in three differently regulated isoforms COX-1, COX-2 and COX-3 [4,6]. COX-1 is a constitutive enzyme which is involved in the production of physiological PGs and TXs that govern the protection of gastric mucosa, normal kidney function and aggregation of platelets, respectively, thereby acting as a "house-keeper" enzyme [3,5,7]. On the other hand, COX-2 is induced at the sites of infection or inflammation as a response to the release of pro-inflammatory mediators and catalyzes the release of pathological PGs involved in the inflammatory process [1,3,7]. In addition, another variant of COX-1 known as COX-3 was discovered in the central nervous system [3,6]. It is to be noted that chronic use of non selective NSAIDs is accompanied by gastrointestinal (GI) complications such as ulceration and bleeding in addition to some renal malfunctions [3,6,8] and these adverse effects are attributed to the inhibition of COX-

* Corresponding author.
*E-mail address:* mai.elshoukrofy@alexu.edu.eg (M.S. El-Shoukrofy).

https://doi.org/10.1016/j.bioorg.2019.02.036
Received 20 November 2018; Received in revised form 15 February 2019; Accepted 17 February 2019
Available online 18 February 2019
0045-2068/ 

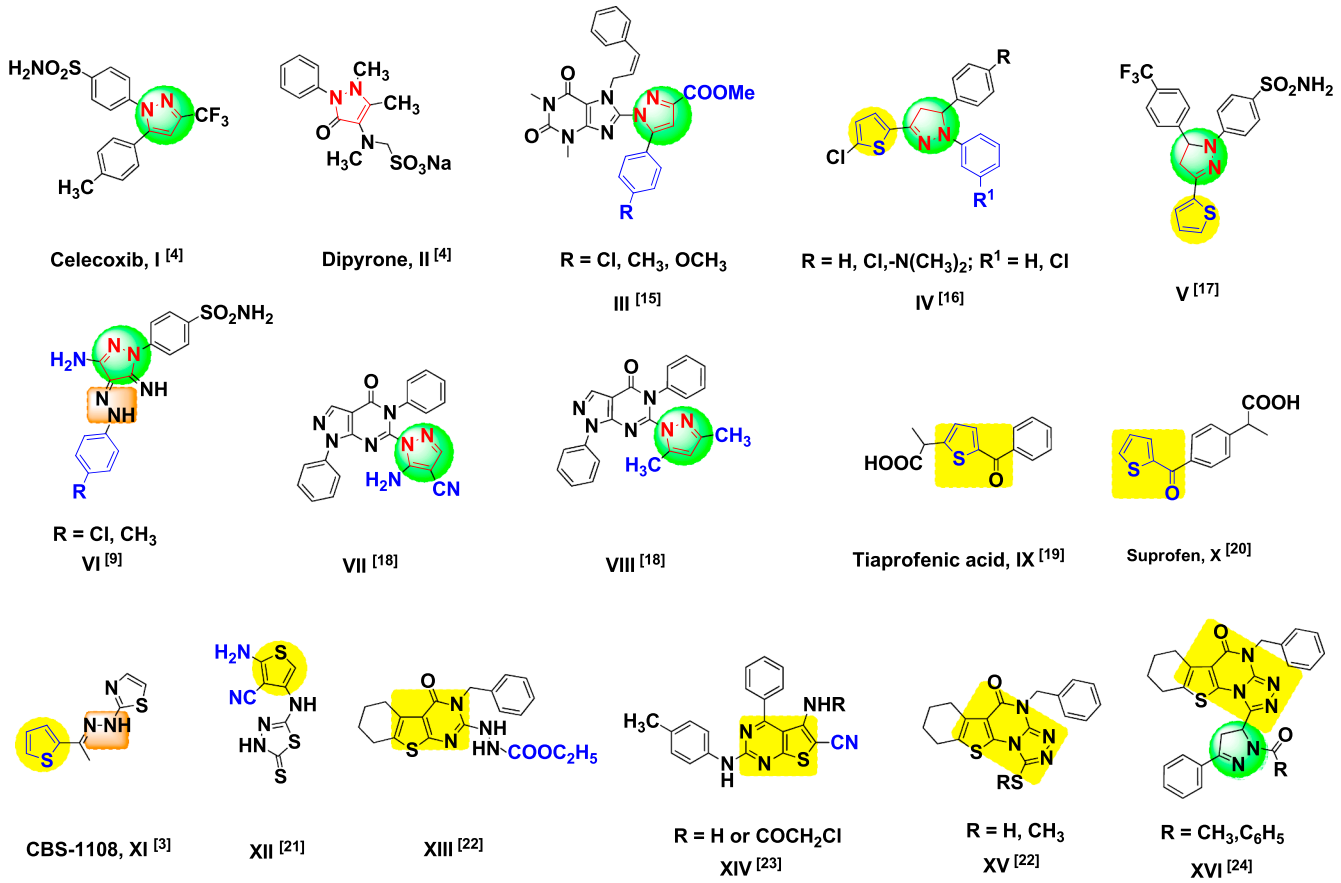


**Fig. 1.** Chemical structures of reported pyrazoles or prazolines **(I-VIII)**, thiophenes **(IX-XII)**, thienopyrimidines or triazolothienopyrimidines **(XIII-XVI)** as anti-inflammatory agents or COX-2 selective inhibitiors.

1 [5,9,10]. Therefore, it was thought that the use of selective COX-2 inhibitors without interfering with COX-1 activity is a fruitful tool for treatment of inflammation with reduced risk of occurrence of side effects especially the GI problems [5–7]. The highly selective COX-2 inhibitors (coxibs) as valdecoxib (Bextra®) and rofecoxib (Vioxx®) that were approved for marketing due to their safe gastrointestinal use [3,5], caused an increased risk of significant cardiovascular (CV) problems upon their administration which led to their withdrawal from the market [1,3,11,12]. On the other hand, moderate selective COX-2 inhibitors like celecoxib (Celebrex®) represent safe anti-inflammatory drugs regarding their cardiovascular effects and are still marketed [12,13]. Unfortunately, the efficacy of celecoxib as an anti-inflammatory agent was not proved in all patients [14]. Thus, the design and synthesis of new COX inhibitors that show appropriate selectivity towards COX-2 inhibition with safe GI profile is a continuous need in order to overcome the CV and GI adverse effects of the currently available COX-2 inhibitors.

Pyrazoles and pyrazolines remain the scaffold of choice for the design of anti-inflammatory agents. Celecoxib (Celebrex®) **I** [4], dipyrone (dimethone ®) **II** [4], compounds **III** [15] and **IV** [16] (Fig. 1) are pyrazole derivatives that exhibited anti-inflammatory activities. Recently, numerous COX-2 selective inhibitors containing pyrazole or pyrazoline moieties have been synthesized (**V-VIII**) [9,17,18] (Fig. 1). The presence of two aryl rings attached to a central pyrazole or pyrazoline moiety is a mutual feature of most COX-2 inhibitors [6]. The nature of substituents on these aryl groups impact the inhibitory potency and selectivity index of the produced COX-2 inhibitor. Phenyl sulfonylamino ($PhSO_2NH_2$) moiety is also a dominant pharmacophore in many selective COX-2 inhibitors with anti-inflammatory properties [3] (compounds **V, VI**). However, the pyrazole core was substituted with other different aryl moieties or attached to them through variable linkages. The trifluoromethylphenylpyrazoles were known as selective COX-2 inhibitors (compound **V** [17]). However, in order to minimize the toxicity risk of fluorine, the trifluoromethyl functionality ($CF_3$) was better replaced with an amino group ($NH_2$) (compound **VI**) [9]. Moreover, pyrazolo[3,4-*d*]pyrimidine moieties (compounds **VII, VIII**) were proved to augment COX-2 selectivity *via* increase in the hydrophobic interactions with COX-2 rather than COX-1 active site [18]. Additionally, 3-aminopyrazole-4-carbonitriles, 3,5-dimethylpyrazoles as well as pyrazoles substituted with an ester or 4-chlorophenyl moieties are well known pharmacophoric scaffolds that improve the anti-inflammatory activity (Fig. 1). Incorporating the hydrazono functionality also showed enhanced COX-2 selectivity (compound **VI**) [9].

It is to be noted that substitution of the pyrazole core with thiophene moiety was also known to yield active anti-inflammatory agents (as in compounds **IV** [16]) or COX-2 selective inhibitors with anti-inflammatory activity (as in compound **V** [17]). In addition, tiaprofenic acid (Surgam ®) **IX** and suprofen (Profenal®) **X** (Fig. 1) are NSAIDs possessing thiophene ring [19,20]. Moreover, CBS-1108 (**XI**) [3] and **XII** [21] are COX-2 selective inhibitors possessing the thiophene pharmacophore incorporating hydrazono functionality or substituted with 2-amino-3-cyano substituents. Furthermore, the tetrahydrobenzothienopyrimidine derivative **XIII** [22] showed increased COX-2 activity with high selectivity index while the thienopyrimidines **XIV** [23] revealed augmented anti-inflammatory activity. Additionally, the triazolothienopyrimidinones **XV, XVI** [22,24] revealed high COX-2 selective inhibition with high selectivity indices.

Strongly convinced by the afore-mentioned studies and tempted by our findings in the field of anti-inflammatory agents [22,24–27], profound interest was developed to access various thiophene pyrazole analogs to be screened for their COX-2 selective inhibition and anti-inflammatory activities (Fig. 2). Our attention has been focused on 2-

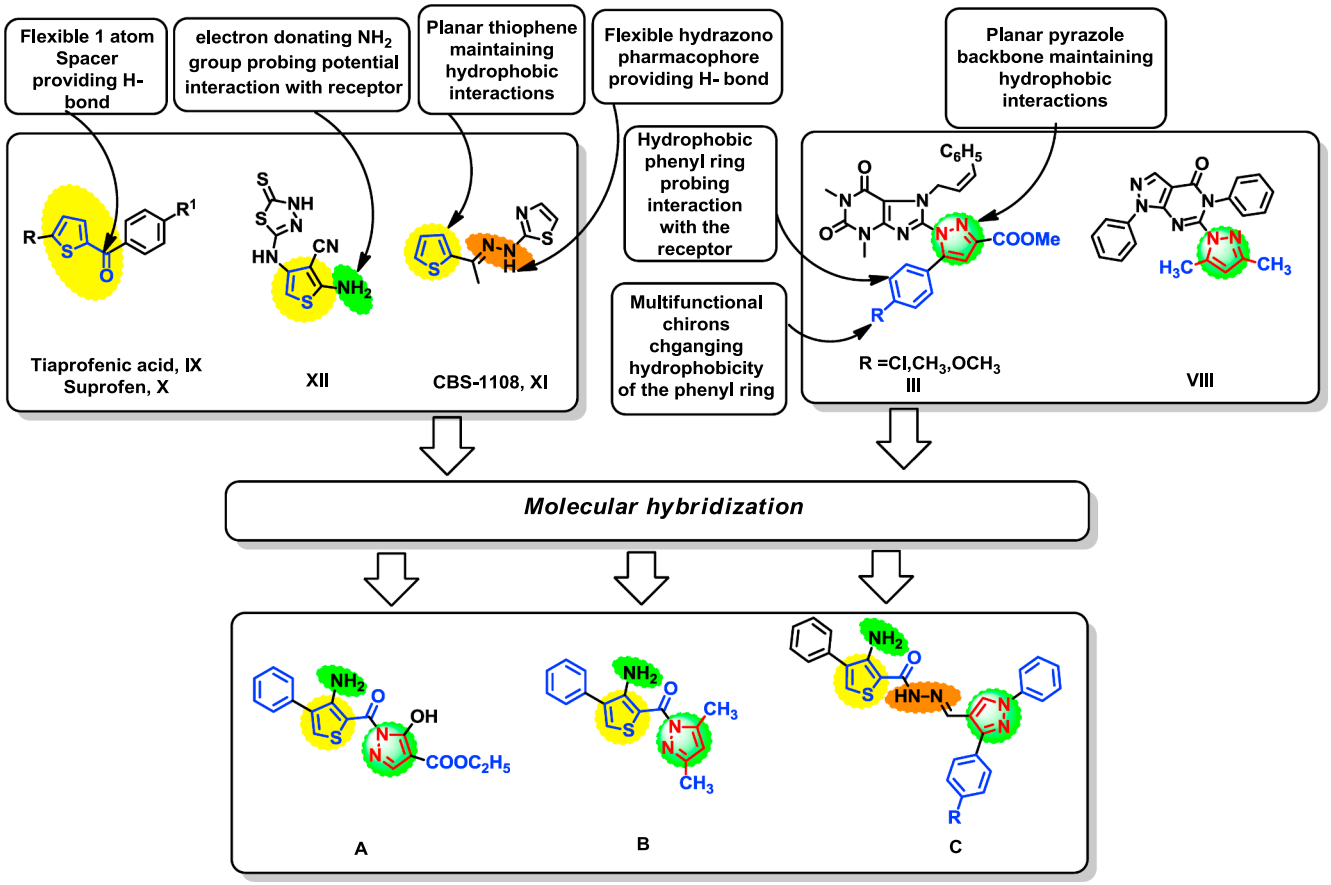


**Fig. 2.** Design of the target thiophene pyrazole hybrids **(A, B and C)**.

aroylthiophene moiety that is a common pharmacophore in many NSAIDs as tiaprofenic acid (**IX**) [19] and suprofen (**X**) [20]. The fact that the electron donating amino group was incorporated in many promising compounds (as **VI** and **VII**), probing probably less toxicity and potential interaction with the receptor was not beyond our interest. Besides, the introduction of phenyl ring implying increased hydrophobicity and interaction with the receptor was also considered. Based on these data and inspired by the well-documented COX-2 selective inhibition and anti-inflammatory activity of the pyrazole ring, a basic scaffold consisting of 3-amino-4-phenyl-2-aroylthiophene was incorporated into variously substituted pyrazole rings either directly (structures **A & B**, Fig. 2) or through a hydrazinomethylene spacer (structure **C**, Fig. 2). Structures **A & B** contain the planar thiophene and pyrazole moieties separated by a flexible one atom spacer (C═O) while structure **C** contains the two aromatic rings separated by a flexible four atom spacer (O═C−NH−N═C) in order to study the effect of such hybridizations on COX-2 selective inhibition and anti-inflammatory activity. Substituents on the pyazole ring include either electron donating groups (hydroxyl or methyl) or electron withdrawing groups (ester or phenyl either unsubstituted or substituted with various chirons) in order to monitor the effect of such substitution on the activity.

Our interest has been also extended to construct two libraries including pyrazole and thieno[3,2-*d*]pyrimidine rings in order to develop new COX-2 selective inhibitors and anti-inflammatory agents. To achieve this interest, the two rings were incorporated into one structure either directly (structure **D**, Fig. 3) or through a three atoms spacer (NH−N═C) (structure **E**, Fig. 3). In addition, it was hypothesized that compounds containing both hydrophobic and hydrophilic components would be promising anti-inflammatory candidates due to variable interactions with receptor binding domain. Thus, variable substituents including amino, cyano, hydroxyl, methyl, ester, phenyl or *p*-chlorophenyl were introduced onto the thieno[3,2-*d*]pyrimidine pyrazole scaffold to study their impact on the anticipated COX-2 selective inhibition and anti-inflammatory activity.

Moreover, it was not beyond our scope to build up the thienotriazolopyrimidine scaffold from the thienopyrimidine ring system and to incorporate such tricyclic ring system directly into the traditional 1,3-diarylpyrazole scaffold (structure **F**, Fig. 3) to study the effect of increasing bulkiness, polarity and restricted rotation of the side chain on the COX-2 selective inhibition and anti-inflammatory activity.

The newly synthesized compounds were evaluated for their *in vitro* COX-1 and COX-2 enzymatic inhibition and their *in vitro* COX-2 selectivity indices were estimated. Moreover, all compounds were evaluated for their *in vivo* anti-inflammatory activities using the formalin-induced paw edema bioassay (acute and sub-acute inflammatory models) and using diclofenac sodium and celecoxib as reference standards. Furthermore, effective concentrations 50 ($ED_{50}$), ulcerogenic activities and acute toxicities ($ALD_{50}$) of the most active compounds in the *in vivo* anti-inflammatory assays were also evaluated and a detailed structure–activity relationship (SAR) study was discussed. Docking of the most active compounds in both *in vitro* and *in vivo* assays into the active site of COX-2 enzyme was performed to predict possible binding modes with the receptor. Computational determination of the *in silico* physicochemical properties of the most active compounds using variable tools was also within our attention.

## 2. Materials and methods

### 2.1. Chemistry

Synthesis of the intermediates and target compounds was

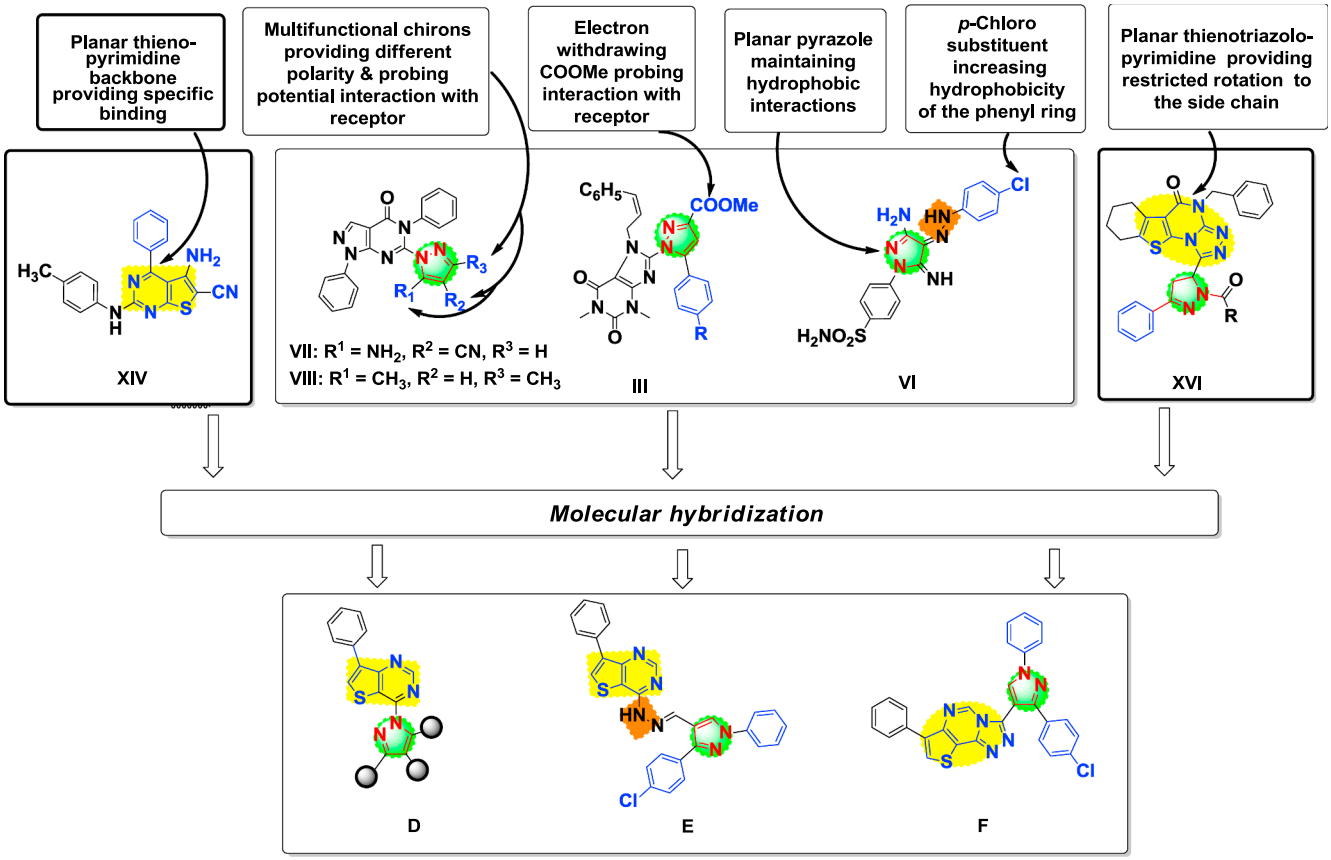


**Fig. 3.** Design of the target thienopyrimidine pyrazole hybrids **(D and E)** & thienotriazolopyrimidine pyrazole hybrid **(F)**.

accomplished according to the steps illustrated in Schemes 1 and 2. The starting material methyl 3-amino-4-phenylthiophene-2-carboxylate **1** [28] was prepared by adding a cold sodium methoxide solution slowly to a mixture of ethyl thioglycolate and 2-cyano-2-phenylvinylbenzenesulfonate and heating the reaction mixture at 60 °C for 2 h following the conditions reported by Lisowski et al. [29]. Treating **1** with hydrazine hydrate 80% yielded 3-amino-4-phenylthiophene-2-carbohydrazide **2** which was used as a precursor for preparation of compounds illustrated in Scheme 1. $^1$H NMR spectrum of compound **2** showed three $D_2O$ exchangeable singlets at 4.33, 6.19 and 7.56 ppm for hydrazino $NH_2$, thiophene $NH_2$ and hydrazino NH protons, respectively in addition to a multiplet integrated for six protons assigned for phenyl and thiophene-$C^5$-Hs. Cyclization of **2** with diethyl ethoxymethylenemalonate was achieved to produce the expected product ethyl 1-(3-amino-4-phenylthiophene-2-carbonyl)-5-hydroxy-1*H*-pyrazole-4-carboxylate **3**. IR spectrum of compound **3** showed two stretching absorption bands at 1693 and 1630 $cm^{-1}$ corresponding to ester and ketonic carbonyl groups in addition to a broad stretching absorption bands at 3483, 3436 and 3345 $cm^{-1}$ for OH and $NH_2$, respectively. $^1$H NMR spectrum of compound **3** revealed the expected triplet and quartet signals assigned for the ethyl moiety at 1.18 and 4.02 ppm, respectively in addition to a new singlet at 7.58ppm for pyrazole-$C^3$-H. The structure was confirmed by EI-MS that demonstrated the molecular ion peak at $m/z$ = 357 in addition to the base peak at $m/z$ = 294.

Reaction of acid hydrazides with ethyl ethoxymethylenecyanoacetate has been previously reported to produce 5-amino-1*H*-pyrazolyl-4-carboxylate derivative [30]. However, in the present work, reacting **2** with ethyl ethoxymethylenecyanoacetate in absolute ethanol produced ethyl 3-(2-(3-amino-4-phenylthiophene-2-carbonyl)hydrazinyl)-2-cyanoprop-2-enoate **4** instead of the expected product. IR spectrum of **4** revealed a sharp peak at 2195 $cm^{-1}$ attributed to cyano group and a broad band at 3443 $cm^{-1}$ due to NH and $NH_2$ functionalities. $^1$H NMR spectrum of compound **4** showed a downfield singlet at 8.37 ppm assigned for =CH. Structure of compound **4** was confirmed using high resolution mass spectrometry where $[M+H]^+$ appeared at 357.099.

On the other hand, condensing **2** with acetylacetone in ethanol gave rise to the corresponding 3,5-dimethylpyrazole **5**. $^1$H NMR spectrum of compound **5** revealed 2 upfield singlets each integrated for 3 protons at 2.24 and 2.51 ppm assigned for 2 methyl groups in addition to a singlet at 6.20 ppm assigned for pyrazole-$C^4$-H.

Moreover, reacting **2** with the appropriate pyrazole-4-carboxaldehyde furnished the corresponding carbohydrazides **6a-c**. $^1$H NMR spectrum of compound **6a** revealed 2 downfield singlets at 8.25 and 8.80 ppm assigned for =CH indicating its existence in Z and E forms in addition to a downfield $D_2O$ exchangeable singlet at 11.19 ppm for NH proton besides the aromatic protons of the newly introduced phenyl rings that resonated as a multiplet and two doublets. EI-MS of compounds **6a** demonstrated the molecular ion peak as the base peak at $m/z$ = 463. $^1$H NMR spectrum of compound **6b** revealed the 4-chlorophenyl protons as two doublets while in the $^1$H NMR spectrum of compound **6c** two of the 4-methylphenyl protons were included within the multiplet attributed for other aromatic protons and the other two resonated as a doublet. The spectrum of compound **6c** also demonstrated an upfield singlet for methyl protons. EI-MS of compound **6c** showed the molecular ion peak at $m/z$ = 477 and the base peak at $m/z$ = 365.

Furthermore, 4-chloro-7-phenylthieno[3,2-*d*]pyrimidine **7** [31] was prepared by heating under reflux a mixture of 7-phenylthieno[3,2-*d*]pyrimidin-4(3*H*)-one and phosphorus oxychloride for 2 h and pouring the reaction mixture onto ice according to the conditions reported by Pédeboscq et al. [32]. Compound **7** was reacted with hydrazine hydrate 99% to give the hydrazinothienopyrimidine **8** which was used as a

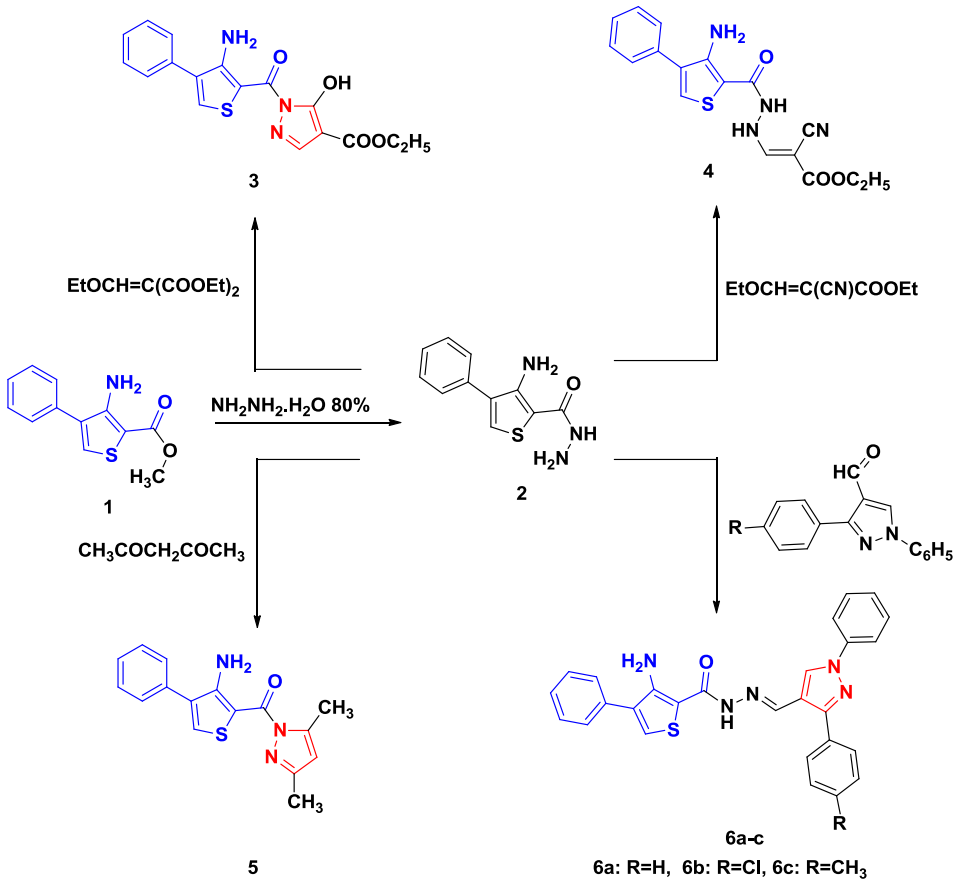


**Scheme 1.** Synthesis of key intermediate **2** and the thiophene pyrazole hybrids **3–6**.

starting material for the target compounds depicted in Scheme 2. $^1$H NMR spectrum of compound **8** demonstrated two $D_2O$ exchangeable singlets for $NH_2$ and NH protons in addition to two downfield singlets at 8.27 and 8.28 ppm for thienopyrimidine-C$^6$ and C$^2$-protons, respectively. Condensation of **8** with ethoxymethylenemalononitrile or ethyl ethoxymethylenecyanoacetate in absolute ethanol, in the presence of anhydrous potassium carbonate resulted in the formation of the corresponding 5-amino-1*H*-pyrazole-4-carbonitrile **9** and 5-amino-1*H*-pyrazole-4-carboxylate **10** derivatives, respectively. $^1$H NMR spectrum of compound **9** showed a broad downfield $D_2O$ exchangeable singlet for $NH_2$ protons in addition to a three downfield singlets for thienopyrimidine-C$^6$-H, pyrazole-C$^3$-H and thienopyrimidine-C$^2$-H, respectively. The same signals were detected in the $^1$H NMR spectrum of compound **10** in addition to a triplet and a quartet for the ethyl group. EI-MS of both compounds demonstrated the molecular ion peak as the base peak at $m/z$ = 318 and 365, respectively.

Analogously, upon reacting **8** with diethyl ethoxymethylenemalonate in refluxing ethanol, the target 5-hydroxy-1*H*-pyrazolyl-4-carboxylate derivative **11** was obtained while reacting **8** with acetylacetone produced 3,5-dimethyl-1*H*-pyrazolyl analog **12**. EI-MS of compound **11** demonstrated the molecular ion peak at $m/z$ = 366 and the base peak at $m/z$ = 320 while $^1$H NMR spectrum of compound **12** revealed 2 new upfield singlets at 2.31 and 2.78 ppm for the 2 methyl groups in addition to a new singlet at 6.31 ppm for pyrazole-C$^4$-H.

Moreover, refluxing **8** with 3-(4-chlorophenyl)-1-phenyl-1*H*-pyrazole-4-carboxaldehyde yielded the corresponding methylenehydrazinylthieno[3,2-*d*]pyrimidine **13** which was reacted with bromine in glacial acetic acid at room temperature to give the unexpected product 8-bromo-3-(3-(4-chlorophenyl)-1-phenyl-1*H*-pyrazol-4-yl)-7-phenylthieno[2,3-*e*][1,2,4]triazolo[4,3-*c*]pyrimidine **14** where cyclization and bromination at C$^8$ occurred. $^1$H NMR spectrum of compound **13** revealed 2 doublets for 4-chlorophenyl protons in addition to a downfield singlet for =CH besides a downfield $D_2O$ exchangeable singlet for NH.$^1$H NMR spectrum of **14** was characterized by the absence of the singlet characteristic for C$^8$ proton and showed a singlet at 9.61 ppm for thienotriazolopyrimidine-C$^5$-H. EI-MS of compound **14** showed $[M^{+\bullet}+4]$ at $m/z$ 586 corresponding to $C_{28}H_{16}{}^{81}Br^{37}ClN_6S$ radical cation, $[M^{+\bullet}+2]$ at $m/z$ 584 corresponding to $C_{28}H_{16}{}^{81}Br^{35}ClN_6S$ or $C_{28}H_{16}{}^{79}Br^{37}ClN_6S$ radical cations and $[M^{+\bullet}]$ at $m/z$ 582 corresponding to $C_{28}H_{16}{}^{79}Br^{35}ClN_6S$ radical cation.

### 2.2. Biological evaluation

#### 2.2.1. In vitro COX-1 and COX-2 enzymatic inhibition assay [33]

All the newly synthesized compounds were evaluated for their *in vitro* inhibition of ovine COX-1 and COX-2 isoenzymes via measuring the peroxidase activity of both enzymes according to the instructions of using Cayman colorimetric COX (ovine) inhibitor screening assay kit. The concentration causing 50% enzyme inhibition ($IC_{50}$, μM) for both enzymes in addition to the *in vitro* COX-2 selectivity indices (SI = $IC_{50}$ COX-1/$IC_{50}$ COX-2) of the test compounds were estimated and recorded in Table 1. Celecoxib and indomethacin were used as reference drugs as examples of selective and non selective COX-2 inhibitors, respectively.

Results revealed that all test compounds elicited weak inhibition of COX-1 isozyme ($IC_{50}$ = 7.52–11.91 μM range) when compared to indomethacin ($IC_{50}$ = 0.10 μM). Compounds **6c, 9, 10** and **13** were weak COX-1 inhibitors with potency close to that of celecoxib ($IC_{50}$ = 10.11–11.91 μM range compared to $IC_{50}$ = 14.70 for celecoxib) expecting that these compounds will have safe gastric profiles.

On the other hand, the newly synthesized compounds showed variable inhibitory activities of COX-2 enzyme. Compound **13** exhibited

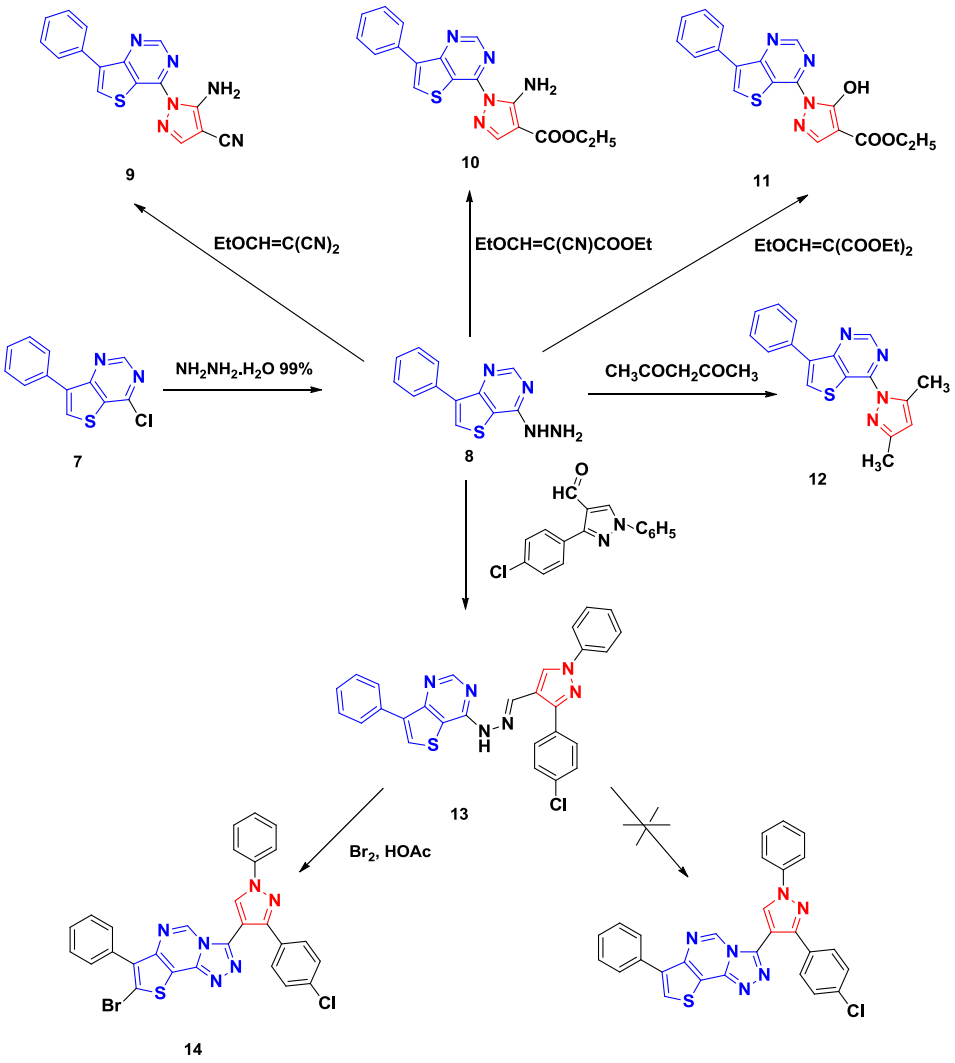


**Scheme 2.** Synthesis of key intermediate **8** and the target compounds **9–14**.

**Table 1**
*In vitro* COX-1 and COX-2 enzymatic inhibition assay results represented as $IC_{50}$ values (μM) and *in vitro* COX-2 selectivity indices (SI) of the newly synthesized compounds and the reference drugs celecoxib and indomethacin.

| Comp. No. | COX-1 $IC_{50}$ (μM)[a] | COX-2 $IC_{50}$ (μM)[a] | COX-2 SI[b] (COX-1/COX-2) |
|---|---|---|---|
| **3** | 7.52 | 0.17 | 44.24 |
| **4** | 8.11 | 0.11 | 73.73 |
| **5** | 8.76 | 0.12 | 73.00 |
| **6a** | 8.61 | 0.12 | 71.75 |
| **6b** | 7.91 | 0.23 | 34.39 |
| **6c** | **10.23** | **0.071** | **144.08** |
| **9** | **10.11** | **0.063** | **160.48** |
| **10** | **11.23** | **0.059** | **190.34** |
| 11 | 9.65 | 0.098 | 98.47 |
| **12** | 7.53 | 0.19 | 39.63 |
| **13** | **11.91** | **0.048** | **248.13** |
| **14** | 7.65 | 0.11 | 69.55 |
| **Celecoxib** | **14.70** | **0.045** | **326.67** |
| **Indomethacin** | 0.10 | 0.080 | 1.25 |

[a] Values are means of three determinations acquired using an ovine COX-1/COX-2 assay kit (catalog no.760111, Cayman Chemicals, MI, USA) and the deviation from the mean is < 10% of the mean value.

[b] *In vitro* COX-2 selectivity index SI (COX-1 $IC_{50}$/COX-2 $IC_{50}$).

COX-2 selective inhibition activity nearly equal to that of celecoxib ($IC_{50}$ = 0.048 μM for **13** and 0.045 μM for celecoxib) while compounds **6c, 9** and **10** exhibited COX-2 selective inhibition activity ($IC_{50}$ = 0.059–0.071 μM range) comparable to that of celecoxib in the order of **10** > **9** > **6c**. Compounds **4, 5, 6a, 11** and **14** demonstrated moderate COX-2 selective inhibition ($IC_{50}$ = 0.098–0.12 μM range) while compounds **3** and **12** showed weak activity with $IC_{50}$ values = 0.17 and 0.19 μM, respectively whereas compound **6b** was the least selective COX-2 inhibitor with $IC_{50}$ = 0.23 μM.

Regarding *in vitro* COX-2 selectivity indices, all test compounds showed relatively higher selectivity towards COX-2 than COX-1 with selectivity indices ranging from 34.39 to 248.13 compared to selectivity indices of 326.67 and 1.25 for celecoxib and indomethacin, respectively. Compound **13** namely, 4-(2-((3-(4-chlorophenyl)-1-phenyl-1*H*-pyrazol-4-yl)methylene)hydrazinyl)-7-phenylthieno[3,2-*d*]pyrimidine elicited the highest COX-2 selectivity index (SI = 248.13) and was moderately selective COX-2 inhibitor. Compounds **6c, 9** and **10** showed also moderate SI in the range of 144.08 to 190.34 in order of **10** > **9** > **6c**.

It is well documented that high COX-2 selectivity causes thrombotic cardiovascular toxicity [3,12] whereas low COX-2 selectivity results in GI problems [5]. Therefore, the thiophene pyrazole derivative **6c** and the thienopyrimidine pyrazole hybrids **9, 10** and **13** are moderately selective COX-2 inhibitors that could act as gastrointestinal safe anti-inflammatory agents.

**Table 2**
*In vivo* anti-inflammatory activities for test compounds, diclofenac sodium and celecoxib in formalin-induced paw edema bioassay (acute inflammatory model) represented as volume of edema (mL) and edema inhibition percentage (EI %).

| Comp. No.[a] | Volume of edema (mL) (mean ± S.E.)[b] | | | | EI % | | |
|---|---|---|---|---|---|---|---|
| | 0 | 1 h | 2 h | 4 h | 1 h | 2 h | 4 h |
| **Control** | 0.30 ± 0.01 | 0.53 ± 0.01 | 0.65 ± 0.01 | 0.69 ± 0.01 | 0 | 0 | 0 |
| **3** | 0.32 ± 0.01 | 0.48 ± 0.02[c] | 0.50 ± 0.02[c] | 0.52 ± 0.02[c] | **61** | **56** | **60** |
| **4** | 0.33 ± 0.02 | 0.51 ± 0.03[c] | 0.57 ± 0.04[c] | 0.63 ± 0.03[c] | 41 | 41 | 30 |
| **5** | 0.33 ± 0.02 | 0.46 ± 0.02[c] | 0.54 ± 0.03[c] | 0.57 ± 0.03[c] | **58** | 48 | 52 |
| **6a** | 0.32 ± 0.01 | 0.43 ± 0.02[c] | 0.45 ± 0.02[c] | 0.50 ± 0.02[c] | **64** | **68** | **64** |
| **6b** | 0.25 ± 0.01 | 0.40 ± 0.02[c] | 0.47 ± 0.02[c] | 0.51 ± 0.02[c] | 51 | 46 | 48 |
| **6c** | 0.34 ± 0.01 | 0.51 ± 0.03[c] | 0.53 ± 0.02[c] | 0.55 ± 0.03[c] | 45 | 53 | **58** |
| **9** | 0.39 ± 0.01 | 0.49 ± 0.02[c] | 0.51 ± 0.01[c] | 0.53 ± 0.01[c] | **67** | **70** | **72** |
| **10** | 0.33 ± 0.02 | 0.48 ± 0.01[c] | 0.53 ± 0.02[c] | 0.55 ± 0.03[c] | 51 | 51 | 56 |
| **11** | 0.34 ± 0.01 | 0.47 ± 0.02[c] | 0.50 ± 0.03[c] | 0.53 ± 0.02[c] | **58** | **60** | **62** |
| **12** | 0.31 ± 0.01 | 0.51 ± 0.03[c] | 0.59 ± 0.03[c] | 0.62 ± 0.03[c] | 35 | 31 | 38 |
| **13** | 0.33 ± 0.01 | 0.52 ± 0.02[c] | 0.54 ± 0.02[c] | 0.63 ± 0.02[c] | 38 | 48 | 30 |
| **14** | 0.31 ± 0.02 | 0.48 ± 0.03[c] | 0.56 ± 0.03[c] | 0.61 ± 0.03[c] | 45 | 39 | 30 |
| **Diclofenac sodium** | 0.30 ± 0.01 | 0.43 ± 0.01[c] | 0.48 ± 0.03[c] | 0.51 ± 0.03[c] | **58** | **56** | **58** |
| **Celecoxib** | 0.33 ± 0.01 | 0.40 ± 0.02[c] | 0.47 ± 0.02[c] | 0.47 ± 0.03[c] | **68** | **60** | **64** |

[a] Dose levels, test compounds and diclofenac sodium (20 mg/kg body weight, *po*).
[b] Values are expressed as mean ± S.E. (n = 5).
[c] Significantly different compared to corresponding control, $p \leq 0.05$.

*2.2.2. In vivo anti-inflammatory activity*

In order to verify results of the *in vitro* COX-1 and COX-2 enzymatic inhibition assay all the newly synthesized compounds were evaluated fore their *in vivo* anti-inflammatory activity using formalin-induced paw edema bioassay (acute and sub-acute inflammatory models) [30,34,35]. Diclofenac sodium and celecoxib were used as reference standards anti-inflammatory agents.

*2.2.2.1. Formalin-induced paw edema bioassay (acute inflammatory model)*. The acute anti-inflammatory activities of all synthesized compounds were evaluated employing formalin-induced paw edema bioassay according to the reported method [30,34] using diclofenac sodium and celecoxib as reference drugs. The paw volume (mL) was measured at zero time and remeasured again 1 h, 2 h and 4 h after administration of formalin. The edema was expressed as an increase in the paw volume and the % of edema inhibition (EI%) was calculated. Results are presented in Table 2, Fig. 4 as the mean paw volume (mean in mL ± S.E.) and edema inhibition percentage (EI %).

The obtained data revealed that test compounds showed a wide range of EI% in the range of 30% to 72% after the three time intervals used. After 1 h, compounds **3**, **6a** and **9** exhibited greater anti-inflammatory activity than diclofenac sodium with activity in the order **9** > **6a** > **3** (EI% = 67%, 64% and 61%, respectively compared to 58% for diclofenac sodium). Meanwhile, compounds **5** and **11** were as effective as diclofenac sodium. However, all compounds demonstrated lower activity than celecoxib except for compounds **9** and **6a** that showed slight comparable activity to celecoxib (EI% = 67% and 64%, respectively compared to EI% = 68% for celecoxib). After 2 h, compounds **6a** and **9** were found to be superior to the two references (EI% = 68% and 70%, respectively compared to EI% = 56% for diclofenac sodium and EI% = 60% for celecoxib). Compound **11** was more potent than diclofenac sodium while eliciting comparable activity to that of celecoxib whereas compound **3** was equipotent to diclofenac sodium with less potency than celecoxib. Taking the 4 h test as a criterion for comparison revealed that compound **9** was more potent than both references with EI % = 72% while compound **6a** displayed similar potency to that of celecoxib and greater activity than diclofenac sodium with EI % = 64%. Similarly, compounds **3** and **11** elicited enhanced activity than diclofenac sodium whereas compound **6c** was as effective as the latter. Other compounds displayed variable activities.

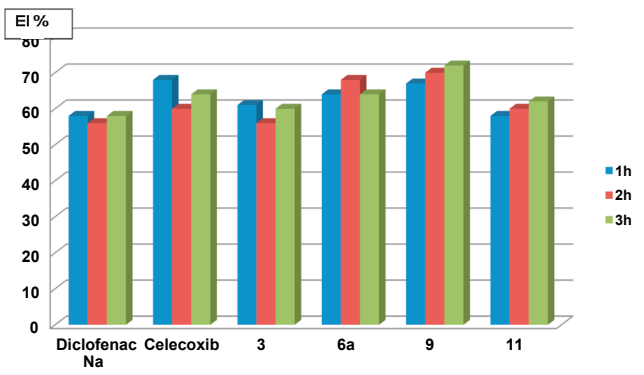


**Fig. 4.** *In vivo* anti-inflammatory activity (EI %) of the most active compounds in the formalin-induced paw edema bioassay (acute inflammatory model).

*2.2.2.2. Formalin-induced paw edema bioassay (sub-acute inflammatory model)*. Sub-acute anti-inflammatory activities of all test compounds were conducted on the rats of the first experiment according to the reported method [34,35]. The changes in the volume of paw were measured on day 1 and day 8. Results are presented in Table 3, Fig. 5 as the mean paw volume (mL, mean ± S.E.) and edema inhibition percentage (EI %).

The obtained data revealed that, on day 1, compounds **3**, **5**, **6a**, **9**, **11** and **13** proved to be more effective than diclofenac sodium with activity in the order **6a** > **5** > **9, 11, 13** > **3** (EI% = 54%, 51%, 48% and 45%, respectively compared to 42% for diclofenac sodium). Meanwhile, compound **10** was found to be as effective as diclofenac sodium while other compounds showed activities noticeably less than that of the latter. In the same context, compound **6a** was more potent than celecoxib while compound **5** was as potent as celecoxib. On day 8, all compounds elicited less activity than that of celecoxib except for compound **9** that showed slight comparable activity to that of celecoxib and was found to be superior over diclofenac sodium (EI% = 58%). Compounds **6c**, **10** and **11** were nearly equipotent to diclofenac sodium with EI% = 51–52%. Other compounds displayed variable activities.

*2.2.2.3. Determination of effective dose 50 ($ED_{50}$) [30]*. Compounds **3, 6a**, **6c**, **9**, **10** and **11** that showed promising *in vivo* anti-inflammatory activities were further tested at 5, 10, 20, 40, and 50 mg/kg body weight and their $ED_{50}$ values were determined by measuring the inhibition of the edema volume 2 h after formalin injection. Results

**Table 3**
*In vivo* anti-inflammatory activities for test compounds, diclofenac sodium and celecoxib in formalin-induced paw edema bioassay (sub-acute inflammatory model) represented as volume of edema (mL) and edema inhibition percentage (EI %).

| Comp. No.[a] | Volume of edema (mL) (mean ± S.E.)[b] | | | EI % | |
|---|---|---|---|---|---|
| | 0 | Day 1 | Day 8 | Day 1 | Day 8 |
| **Control** | 0.30 ± 0.01 | 0.63 ± 0.02 | 0.85 ± 0.02 | 0 | 0 |
| **3** | 0.32 ± 0.01 | 0.50 ± 0.02[c] | 0.61 ± 0.01[c] | **45** | 47 |
| **4** | 0.33 ± 0.02 | 0.55 ± 0.01[c] | 0.73 ± 0.04[c] | 33 | 26 |
| **5** | 0.33 ± 0.02 | 0.49 ± 0.02[c] | 0.61 ± 0.02[c] | **51** | 49 |
| **6a** | 0.32 ± 0.01 | 0.47 ± 0.02[c] | 0.60 ± 0.02[c] | **54** | 49 |
| **6b** | 0.25 ± 0.01 | 0.46 ± 0.02[c] | 0.55 ± 0.02[c] | 36 | 45 |
| **6c** | 0.34 ± 0.01 | 0.57 ± 0.03[c] | 0.60 ± 0.03[c] | 30 | **52** |
| **9** | 0.39 ± 0.01 | 0.56 ± 0.02[c] | 0.62 ± 0.04[c] | **48** | **58** |
| **10** | 0.33 ± 0.02 | 0.52 ± 0.02[c] | 0.60 ± 0.03[c] | **42** | **51** |
| **11** | 0.34 ± 0.01 | 0.51 ± 0.01[c] | 0.60 ± 0.03[c] | **48** | **52** |
| **12** | 0.31 ± 0.01 | 0.55 ± 0.03[c] | 0.64 ± 0.02[c] | 27 | 39 |
| **13** | 0.33 ± 0.01 | 0.51 ± 0.02[c] | 0.63 ± 0.02[c] | **48** | 45 |
| **14** | 0.31 ± 0.02 | 0.56 ± 0.01[c] | 0.66 ± 0.02[c] | 24 | 35 |
| **Diclofenac sodium** | 0.30 ± 0.01 | 0.49 ± 0.01[c] | 0.55 ± 0.03[c] | **42** | **54** |
| **Celecoxib** | 0.33 ± 0.01 | 0.49 ± 0.01[c] | 0.54 ± 0.02[c] | **51** | **61** |

[a] Dose levels, test compounds and diclofenac sodium (20 mg/kg body weight, *po*).
[b] Values are expressed as mean ± S.E. (n = 5).
[c] Significantly different compared to corresponding control, $p \leq 0.05$.

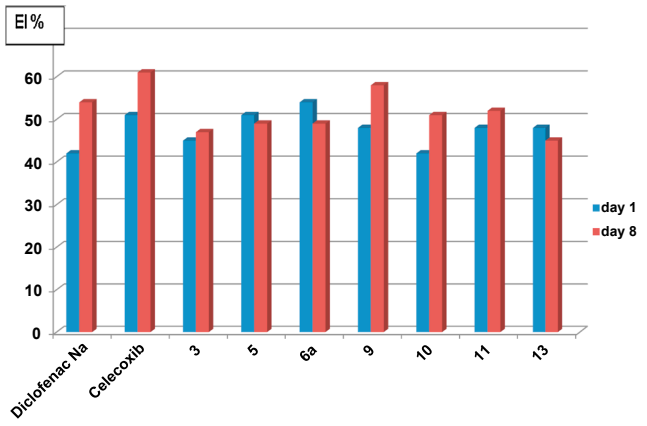


**Fig. 5.** *In vivo* anti-inflammatory activity (EI %) of the most active compounds of the formalin-induced rat paw edema bioassay (sub-acute inflammatory model).

**Table 4**
Effective dose 50 ($ED_{50}$) (mmol/kg), ulcerogenic effects (% ulceration) and acute $LD_{50}$ (mg/kg) for compounds **3, 6a**, **6c**, **9**, **10** and **11**.

| Comp. No. | $ED_{50}$[a] (mmol/kg) | % Ulceration[b,c] | $ALD_{50}$ (mg/kg) |
|---|---|---|---|
| **3** | 0.045 | 10.0 | > 400 |
| **6a** | 0.033 | 10.0 | > 400 |
| **6c** | 0.035 | 0.0 | > 400 |
| **9** | 0.038 | 0.0 | > 400 |
| **10** | 0.048 | 10.0 | > 400 |
| **11** | 0.042 | 0.0 | > 400 |
| **Diclofenac sodium** | 0.052 | 0.0 | – |
| **Celecoxib** | 0.041 | 0.0 | – |
| **Indomethacin** | – | 100 | – |

[a] Effective dose calculated 2 h after formalin injection.
[b] Dose levels, *po*: test compounds (20 mg/kg b.wt.).
[c] Values are expressed as mean ± S.E. (n = 5).

are presented in Table 4 as $ED_{50}$ (mmol/kg) and revealed that all compounds displayed greater potency than diclofenac sodium with $ED_{50}$ = 0.033–0.048 mmol/kg range compared to $ED_{50}$ = 0.052 mmol/kg for diclofenac sodium. On the other hand, compounds **6a**, **6c** and **9** showed superior potency than celecoxib while compound **11** was slightly equipotent to celecoxib. Other compounds were less potent than celecoxib. The potency was in the order **6a** > **6c** > **9** > **11** > **3** > **10** (Fig. 6) with compound **6a** being the most potent showing $ED_{50}$ = 0.033 mmol/kg.

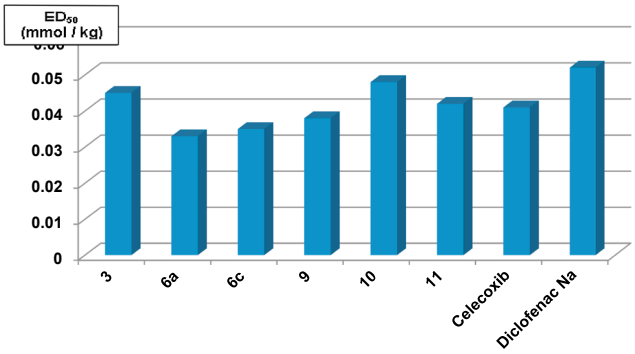


**Fig. 6.** Effective dose 50 ($ED_{50}$) (mmol/kg) for compounds **3, 6a**, **6c**, **9**, **10** and **11**.

*2.2.2.4. Determination of ulcerogenic activity*. Compounds **3**, **6a**, **6c**, **9**, **10** and **11** that exhibited pronounced *in vivo* anti-inflammatory profiles were further evaluated for their ulcerogenic potential in rats according to the reported method [36] using diclofenac sodium, indomethacin and celecoxib as reference standards. Results are presented in Table 4 as % ulceration. Gross observation of the isolated rat stomachs showed a normal stomach texture for compounds **6c**, **9** and **11** with no observable hyperemia indicating a superior GI safety profile in the population of the test animals. On the other hand, compounds **3**, **6a** and **10** showed weak ulcerative effect (10%) compared to both celecoxib and diclofenac sodium (no ulceration). All test compounds were less ulcerogenic than indomethacin that showed 100% ulceration.

*2.2.2.5. Determination of acute toxicity*. The most active compounds (**3**, **6a**, **6c**, **9**, **10** and **11**) were further evaluated for their approximate acute lethal dose ($ALD_{50}$) using a literature method [37]. Results are presented in Table 4 indicating that all test compounds proved to be non-toxic and were well tolerated by the experimental animals. Test compounds showed a high safety margin when screened at graded doses 100–400 mg/kg, *po*, where their $ALD_{50}$ values were found to be > 400 mg/kg.

*2.2.2.6. Structure-Activity Relationship (SAR) study of the in vivo anti-inflammatory activities results:*.

- A collective interpretation of the *in vivo* anti-inflammatory activity of the test compounds in the pre-mentioned screens Tables 2 and 3 revealed that the thiophene pyrazole hybrids **3**, **6a** and **6c** in addition to the thienopyrimidine pyrazole derivatives **9**, **10** and **11** showed pronounced activity in the formalin-induced paw edema screen (both the acute and sub-acute models). These facts would suggest that such type of compounds might be effective in managing chronic as well as acute inflammatory conditions.
- Inspection of the structures of the test compounds revealed that within the tested thiophene pyrazole hydrids, compound **3** containing 5-hydroxypyrazole-4-carboxylate moiety attached to the thiophene ring through a carbonyl group was more active than diclofenac sodium especially in the acute inflammatory model while being less potent than celecoxib in both models.
- Replacement of the 5-hydroxypyrazole-4-carboxylate moiety by dimethylpyrazole ring system in compound **5** decreased the *in vivo* acute anti-inflammatory activity while its sub-acute anti-

inflammatory activity was increased especially on day 1 of the sub-acute anti-inflammatory assay.

- Introduction of diarylpyrazole functionality separated from the aminothiophene ring by 4 atoms spacer produced variable activities. Compound **6a** (R = H) was found to be more active or of comparable activity to both reference standards especially in the acute inflammatory model and on day 1 of the sub-acute anti-inflammatory assay. In addition, compound **6c** (R = $CH_3$) was equipotent to diclofenac sodium after 4 h of formalin injection while compound **6b** (R = Cl) exhibited the least *in vivo* anti-inflammatory activity within this series.
- Among the five tested thienopyrimidine derivatives, compound **9** containing aminopyrazolecarbonitrile moiety proved to be the most active in the *in vivo* acute and sub-acute inflammatory models.
- Replacement of the carbonitrile moiety with carboxylate functionality in compound **10** decreased the *in vivo* anti-inflammatory activity in both models.
- Replacement of the amino group in compound **10** with hydroxyl group (compound **11**) increased the *in vivo* anti-inflammatory activity in both models. However, the introduction of either dimethylpyrazole (compound **12**) or diarylpyrazole functionality (compound **13**) decreased the *in vivo* anti-inflammatory activity especially in the acute model.
- Thienotriazolopyrimidine derivative **14** was less active than its thienopyrimidine precursor **13** in both models.

*2.2.2.7. Statistical analysis*. Data obtained are presented as means ± S.E. of the mean. The concentration-dependent effects of various drugs *in vitro* were evaluated statistically by the randomized block design analysis of variance (ANOVA) followed by Student-Newman-Keuls Multiple Comparison Test. The difference in results was considered significant when $p < 0.05$.

### 2.2.3. In silico studies

*2.2.3.1. Docking studies*. Further, to determine the plausible modes of binding of the most active compounds in both *in vitro* and *in vivo* assays with COX-2 enzyme, molecular docking studies of compounds **3, 6a, 6c, 9, 10, 11** and **13** were performed using Molecular Operating Environment (MOE) version 2014.09 [38]. Crystal structure of COX-2 complexed with celecoxib (PDB code 3LN1) [39] was retrieved from the Protein Data Bank. Docking scores, amino acid residues forming hydrophobic or hydrogen bonding interactions and their lengths were summarized in Table 5.

Regarding COX-2 enzyme, Celecoxib sulfonyl moiety ($SO_2$) and 4-tolyl ring made one H-bonding interaction with His 200 amino acid and one arene–arene interaction with His 374 amino acid in a distance of 3.60 and 3.97 Å, respectively with an energy score equals to-5.05 kcal/Mol.

Compounds that were subjected to molecular docking fitted well to COX-2 active site inside the pocket and showed good binding energy scores ranged from −5.17 to − 8.60 kcal/Mol. Docking results revealed that compounds **3, 6a, 10, 11** and **13** showed arene–arene interaction with His 374 amino acid while compounds **6c** and **9** exhibited arene-cation interaction with the same amino acid residue indicating that all test compounds shared pretty similar binding mode with celecoxib. Compound **6c** showed H-bonding interaction with His 200 amino acid similar to that of celecoxib while compounds **10** and **13** demonstrated H-bonding interactions with Thr 198 amino acid. Compounds **6a** and **13** showed arene-cation interaction with His 200 amino acid while compounds **3, 6c**, **11** and **13** revealed additional arene-cation interaction with His 372 amino acid. On the other hand, the docking poses of compounds **6c, 9, 10** and **13** that elicited the highest *in vitro* COX-2 selectivity indices, appeared to access more residues in the binding site of COX-2 enzyme compared to the co-crystallized ligand. Compound **6c** revealed a third arene-cation interaction with Lys 197 while compound **10** exhibited a second arene-cation interaction with Trp 373 amino acid. Furthermore, both compounds **9** and **13** showed two additional arene-cation interactions with Gln 189 and His 193 amino acids for compound **9** and with Gln 189 amino acid for compound **13**. Therefore, docking studies results proved that all test compounds showed high binding affinity to COX-2 enzyme in addition to promising binding patterns comparable to that of celecoxib. The proposed binding modes and 2D interactions of celecoxib and compounds **3, 6a, 6c, 9, 10, 11** and **13** with amino acid residues in COX-2 receptor active site (PDB code 3LN1) were presented in Figs. 7A and 7B while their proposed 3D interactions were demonstrated in Figs. 8A and 8B.

*2.2.3.2. In silico Chemo-informatic properties evaluation*. Bioavailability is a factor that must be considered in clinical applications. It is affected by the physicochemical properties of compounds including molecular weight, fat-water partition coefficient and others [40]. In an attempt to explain the different behavior of the newly synthesized ligands in the *in vitro* and *in vivo* assays, the most active ligands in both screenings namely, compounds **3, 6a, 6c, 9, 10, 11** and **13** were analyzed computationally to predict the best ligand on the basis of Lipinski's rule of five (RO5), chemical and bio-molecular properties. In this study, Molinspiration tool [41] is used to predict the drug-likeness properties of the most active ligands and their violations from Lipinski's RO5 [42–44]. Moreover, the % absorption (% ABS) of compounds **3, 6a, 6c, 9, 10, 11** and **13** were calculated [44]. The solubility (Mol log S in mg/L) and the drug likeness model score of the most active compounds were predicted using Molsoft software [45,46]. Furthermore, the predicted human intestinal absorption (HIA), blood–brain barrier penetration (BBB) and plasma protein binding (PPB) were evaluated by Pre ADMET calculator [47] to evaluate the overall pharmacokinetic profile of the compounds. The predicted chemo-informatic properties are mentioned in Table 6.

Lipinski's RO5 refers to four physicochemical properties of a molecule to become a drug, i.e. molecular weight (MW) should be < 500, logP < 5, H-bond donors < 5 and H-bond acceptor < 10. Compounds that comply or show only one violation from Lipinski's RO5 were known to exhibit good oral bioavailability and were suitable for oral administration [42,43]. Results revealed that compounds **3, 9, 10** and **11** comply with Lipinski's RO5 with no violations while compounds **6a** and **6c** show only 1 violation whereas compound **13** demonstrated 2 violations from Lipinski's RO5. This can explain the difference between the *in vivo* and *in vitro* screenings results of these compounds. Test compounds were administered orally during the *in vivo* anti-inflammatory assays so oral bioavailability will reflect on the *in vivo* results. Therefore, compounds **3, 6a, 6c, 9, 10** and **11**, complying with RO5, exhibited variable *in vivo* anti-inflammatory activities. On the other hand, compound **13**, the most active compound in the *in vitro* COX-1 and COX-2 enzymatic inhibition assay, did not show remarkable *in vivo* anti-inflammatory activity as it showed 2 violations from Lipinski's RO5, i.e. has certain bioavailability problems.

Another factor that affect drug bioavailability is the topological polar surface area (TPSA) of the compound where passively absorbed compounds with a TPSA > 140 $Å^2$ are thought to have low oral bioavailability [48]. All compounds showed acceptable TPSA results in the range of 68.00–107.45 $Å^2$. Moreover, all compounds were predicted to display good % absorption in the range of 71.93–85.54%. Furthermore, all compounds could be well absorbed across the intestinal epithelium (HIA > 91%) while they were predicted to have weak blood brain barrier penetration (BBB**:** 0.06–0.22). In addition, compounds **3, 9, 10** and **11** showed high affinity to plasma protein (PPB: 88–96%) while compounds **6a, 6c** and **13** showed 100% PPB. This parameter may also account for their diminished *in vivo* anti-inflammatory activities compared with the promising *in vitro* results. In addition, compounds **6a, 6c** and **13** were insoluble in water (mol log S = 0) while other compounds displayed good water solubility (0.19–0.56). Predicted drug likeness model scores revealed that the best score was for compound **11**

**Table 5**
The docking scores and proposed binding interactions of compounds **3, 6a, 6c, 9, 10, 11** and **13** inside COX-2 active site.

| Comp. No. | Docking scores (Kcal/mol) | Hydrogen bonding | | Other interactions | |
|---|---|---|---|---|---|
| | | Residues involved (distance Å) | Functional group | Residues involved (distance Å) | Functional group |
| **Celecoxib** | −5.0500 | His 200 (3.60) | $SO_2$-*O* | Arene-arene His 374 (3.97) | *p*-tolyl ring |
| **3** | −5.8330 | – | – | Arene-arene His 374 (4.00)<br>Arene-cation His 372 (3.71) | Thiophene ring<br>Thiophene-$NH_2$ |
| **6a** | −6.3438 | – | – | Arene-arene His 374 (3.88)<br>Arene-cation His 200 (3.48) | Thiophene ring<br>Pyrazole ring |
| **6c** | −8.6037 | His 200 (3.34) | Pyrazole-*N*2 | Arene-cation His 374 (4.08)<br>Arene-cation Lys 197 (4.32)<br>Arene-cation His 372 (4.24) | Phenyl-$C^2$<br>Pyrazole ring<br>Thiophene ring |
| **9** | −5.8014 | – | – | Arene-cation His 374 (3.26)<br>Arene-cation Gln 189 (3.90)<br>Arene-cation His 193 (3.28) | Pyrimidine ring<br>Phenyl ring<br>Pyrimidine ring |
| **10** | −5.1697 | Thr 198 (2.97) | Carbonyl-*O* | Arene-arene His 374 (3.89)<br>Arene-cation Trp 373 (4.38) | Thiophene ring<br>Phenyl ring |
| **11** | −5.9462 | – | – | Arene-arene His 374 (3.87)<br>Arene-cation His 372 (4.09) | Pyrimidine ring<br>Pyrazole ring |
| **13** | −8.2479 | Thr198 (2.94) | *N*1-thienopyrimidine ring | Arene-arene His 374 (3.80)<br>Arene-cation His 372 (3.91)<br>Arene-cation His 200 (4.20)<br>Arene-cation Gln 189 (4.31)<br>Arene-cation Gln 189 (3.73) | Pyrazole ring<br>NH<br>Thiophene ring<br>Pyrazole ring<br>Phenyl ring |

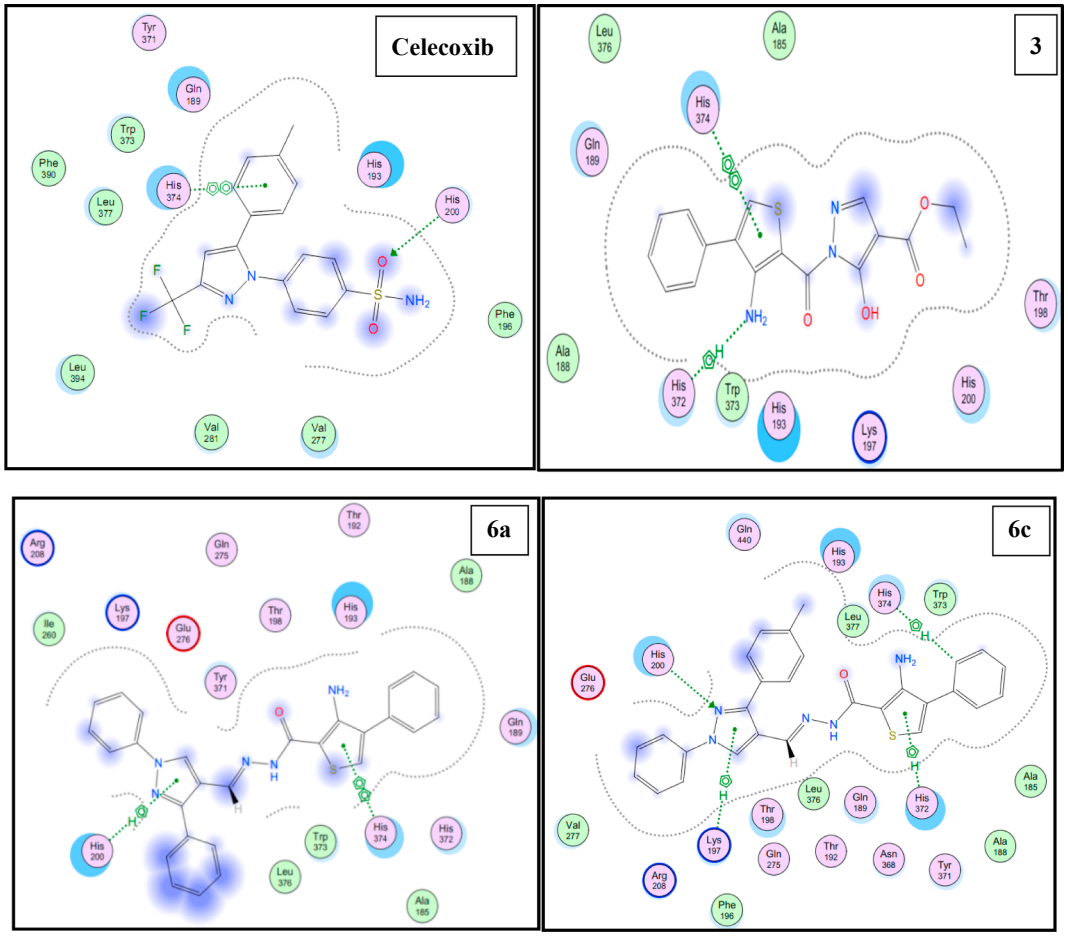


**Fig. 7A.** The proposed 2D interactions of celecoxib and compounds **3, 6a** and **6c** with amino acids residues in COX-2 receptor active site (PDB code 3LN1).

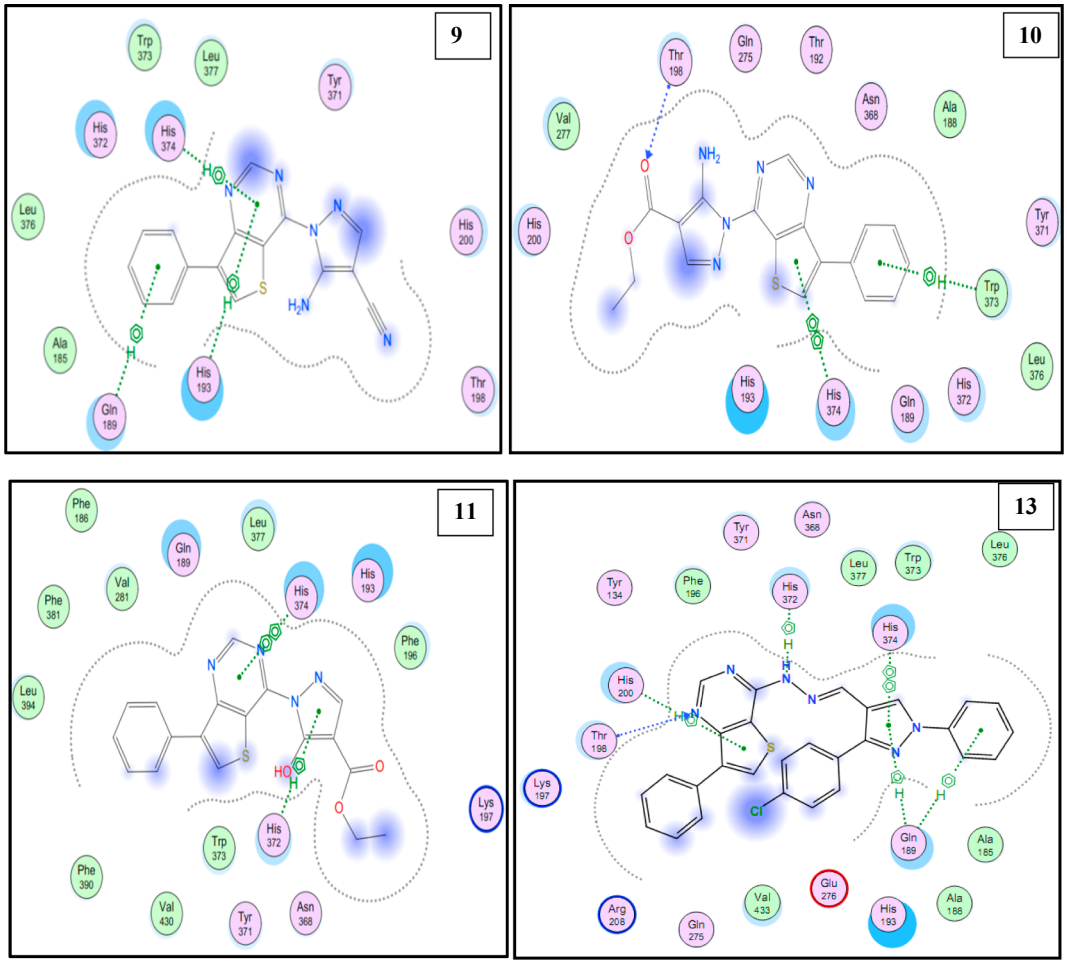


**Fig. 7B.** The proposed 2D interactions of compounds **9, 10, 11** and **13** with amino acids residues in COX-2 receptor active site (PDB code 3LN1).

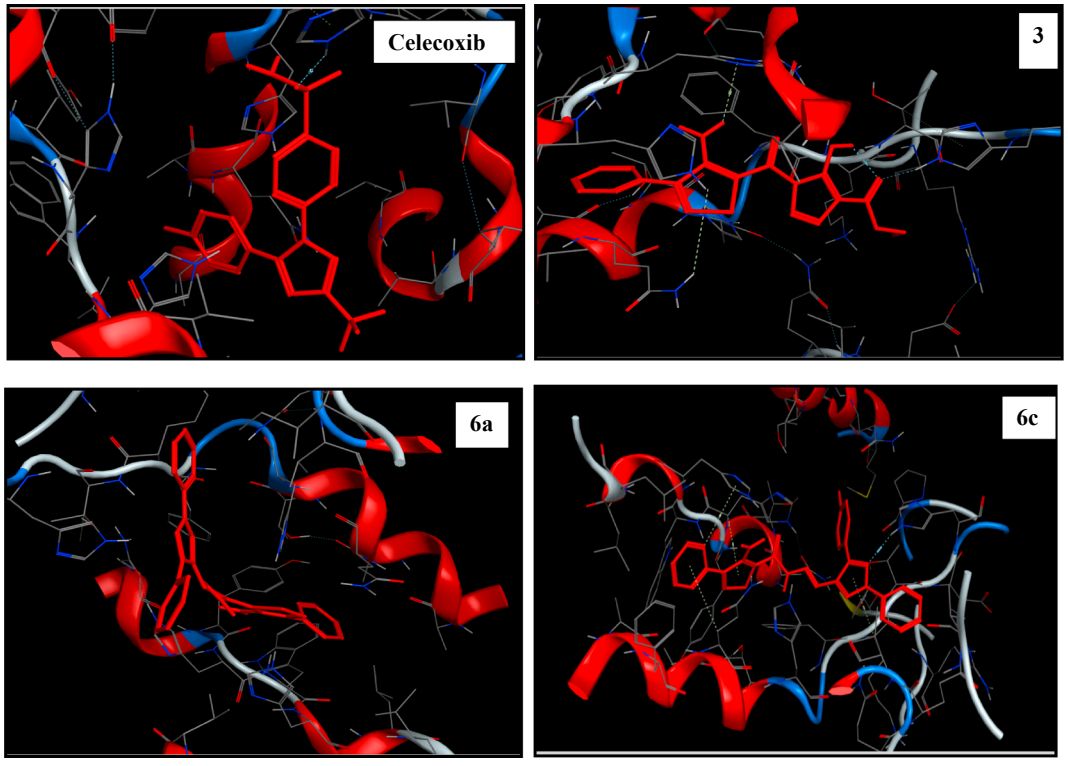


**Fig. 8A.** The proposed 3D interactions of celecoxib and compounds **3, 6a** and **6c** with amino acids residues in COX-2 receptor active site (PDB code 3LN1).

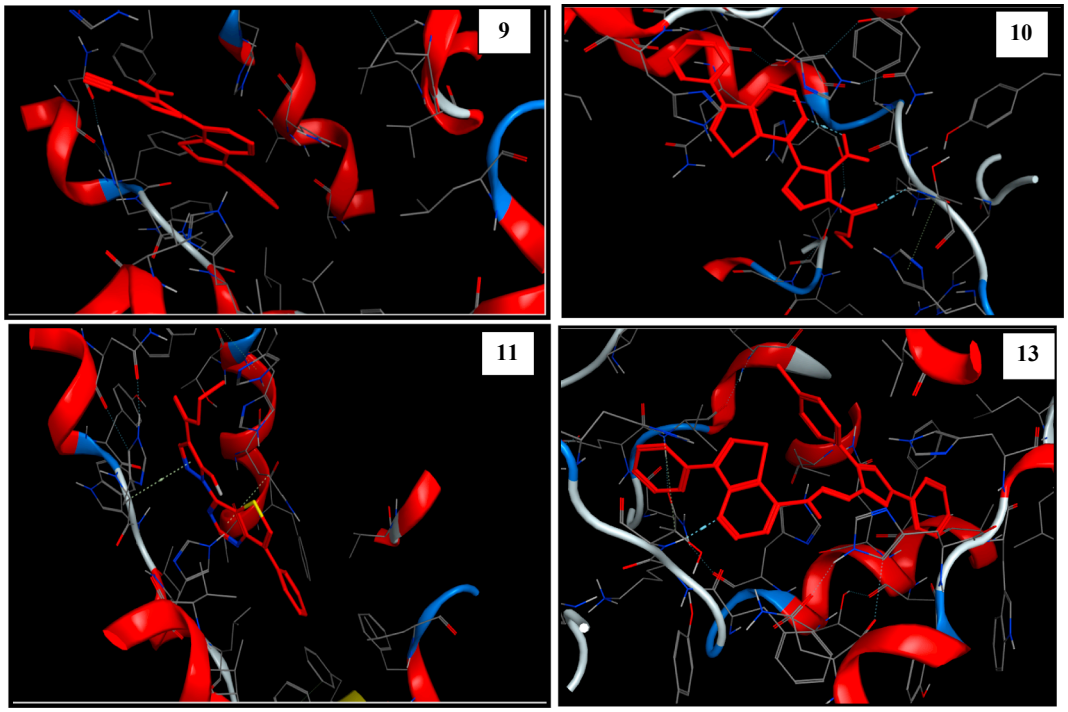


**Fig. 8B.** The proposed 3D interactions of compounds **9, 10, 11** and **13** with amino acids residues in COX-2 receptor active site (PDB code 3LN1).

followed by compounds **10** and **3** (Drug likeness model score = 0.78, 0.67 and 0.54, respectively) indicating that these compounds displayed acceptable drug-likeness parameters and are suitable anti-inflammatory candidates that can be orally administered.

## 3. Conclusion

Design and synthesis of new thiophene - pyrazole hybrids were achieved. All compounds were found to be more COX-2 selective inhibitors than COX-1 with compound **13** exhibiting activity nearly equal to that of celecoxib and compounds **6c, 9** and **10** eliciting comparable activity to that of celecoxib in the order of **10** > **9** > **6c**. Selectivity indices of compounds **6c, 9, 10** and **13** revealed that they are moderately selective COX-2 inhibitors. Acute *in vivo* anti-inflammatory assays showed that compounds **3, 6a, 9** and **11** were the most active. Compounds **5** and **6a** were the most active on day 1 of the sub-acute anti-inflammatory assay compared to celecoxib while compounds **3, 5, 6a, 6c, 9, 10, 11 a**nd **13** elicited promising activity superior or comparable to that of diclofenac sodium on day 1 and / or day 8. Compounds **3, 6a**, **6c**, **9**, **10** and **11** were further tested for their $ED_{50}$ values where compounds **6a**, **6c** and **9** showed higher potency than celecoxib while all compounds were more potent than diclofenac sodium with compound **6a** being the most potent showing $ED_{50}$ = 0.033 mmol/kg. Compounds **6c**, **9** and **11** showed gastrointestinal safety profile comparable to that of celecoxib and diclofenac sodium in the ulcerogenic assay while compounds **3, 6a**, **6c**, **9**, **10** and **11** were non-toxic and well tolerated by the experimental animals. In an attempt to explain the different behavior of the newly synthesized ligands in the *in vitro* and *in vivo* assays, the most active ligands in both screenings namely, compounds **3, 6a, 6c, 9, 10, 11** and **13** were docked into COX-2 receptor active site. Test compounds showed high binding affinity to COX-2 enzyme with binding energy scores comparable to that of celecoxib. The docking poses of compounds **6c, 9, 10** and **13** that elicited the highest *in vitro* COX-2 selectivity indices, appeared to access more residues in the binding site of COX-2 enzyme compared to the co-crystallized ligand. Other compounds showed binding modes analogous to that of celecoxib. Chemo-informatic properties of compounds **3, 6a, 6c, 9, 10, 11** and **13** were predicted and results were compared with the biological results. Compounds **3, 6a, 6c, 9, 10** and **11**, complying with Lipinski's RO5, exhibited variable *in vivo* anti-inflammatory activities. However, compound **13** showed 2 violations from Lipinski's RO5 while compounds **6a, 6c** and **13** showed 100% plasma protein binding (PPB) and no aqueous solubility (mol log S = 0) accounting for their variable *in vivo* anti-inflammatory activities compared with the promising *in vitro* results. Predicted drug likeness model scores revealed that the best score was for compounds **3, 10** and **11**. A deep insight into the structure of these compounds confirmed that thiophene or thienopyrimidine rings

**Table 6**
Chemo-informatic analyses of compounds **3, 6a, 6c, 9, 10, 11** and **13**.

| Comp. No. | Molinspiration | | | | | | | Pre ADMET | | | Molsoft | |
|---|---|---|---|---|---|---|---|---|---|---|---|---|
| | Log*P* | MW | *n*-ON | *n*-OHNH | Lipinski's Violation | TPSA (Å$^2$) | % ABS | PPB% | BBB | HIA% | Mol log S (mg/L) | Drug likeness model score |
| **3** | 2.93 | 357.39 | 7 | 3 | 0 | 107.45 | 71.93 | 87.61 | 0.06 | 91.55 | 0.56 | 0.54 |
| **6a** | **5.46** | 463.57 | 6 | 3 | 1 | 85.31 | 79.57 | 100.00 | 0.09 | 96.17 | 0.00 | 0.08 |
| **6c** | **5.91** | 477.59 | 6 | 3 | 1 | 85.31 | 79.57 | 100.00 | 0.09 | 96.27 | 0.00 | 0.40 |
| **9** | 2.58 | 318.37 | 6 | 2 | 0 | 93.42 | 76.77 | 96.47 | 0.11 | 97.84 | 0.19 | −0.33 |
| **10** | 3.03 | 365.42 | 7 | 2 | 0 | 95.94 | 75.90 | 88.94 | 0.17 | 98.14 | 0.26 | 0.67 |
| **11** | 3.33 | 366.40 | 7 | 1 | 0 | 90.14 | 77.90 | 95.31 | 0.22 | 97.89 | 0.25 | 0.78 |
| **13** | **6.44** | **507.02** | 6 | 1 | 2 | 68.00 | 85.54 | 100.00 | 0.08 | 97.79 | 0.00 | 0.35 |

directly attached or separated with one atom spacer from a pyrazole moiety substituted at the 4-position with an ester functionality is a promising scaffold for the design of novel biologically active anti-inflammatory ligands having moderate COX-2 selectivity and hence safe gastrointestinal and cardiovascular profiles. Therefore, the thiophene analog **3** and the thienopyrimidine derivatives **10** and **11** are considered promising non-toxic, gastrointestinal safe anti-inflammatory candidates with moderate COX-2 selectivity, good oral bioavailability and physicochemical properties.

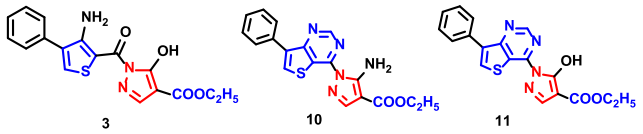


## 4. Experimental

### 4.1. Chemistry

All reagents and solvents were purchased from commercial suppliers and were dried and purified when necessary by standard techniques. Melting points were determined in open glass capillaries on a Stuart capillary melting point apparatus (Stuart scientific Stone, Staffordshire, UK) and were uncorrected. The infrared (IR) spectra were recorded on Perkin-Elmer 1430 infrared spectrophotometer (PerkinElmer, Beaconsfield, UK) using the KBr plate technique, (ύ, $cm^{-1}$). Nuclear magnetic resonance ($^1H$ and $^{13}C$ NMR) were scanned on Jeol 500 MHz spectrometer (Faculty of Science, Alexandria University and National Research Center, Dokki, Cairo, Egypt), on a Mercury 300 MHz spectrophotometer (Faculty of Science, Cairo University, Egypt) and on Bruker Avance III FT-NMR 400 MHz spectrophotometer (Faculty of Pharmacy, University of Kafr Elshiekh, Egypt) using tetramethylsilane (TMS) as the internal standard and DMSO-$d_6$ as the solvent (chemical shifts in $\delta$, ppm). High resolution mass spectra (HRMS) were run in positive mode on AB SCIEX Triple Quad$^{TM}$5500 LC/MS/MS (City for Scientific Research & Technology, Alexandria, Egypt). Electron impact mass spectra (EI-MS) were carried out using a Schimadzu gas chromatograph/mass spectrophotometer GCMS-QP-2010 Plus (70ev), Faculty of Science, Cairo University, Egypt. Elemental Microanalyses were performed at the regional center for Mycology and Biotechnology, Al-Azhar University and at the Microanalytical Unit, Faculty of Science, Cairo University, Egypt. Values were within ± 0.4% of the theoretical values. Follow up of the reactions and checking the homogeneity of the compounds were made by TLC on silica gel-protected glass plates and the spots were detected by exposure to UV-lamp at λ 254 nm for few seconds.

#### 4.1.1. 3-Amino-4-phenylthiophene-2-carbohydrazide (2)

A mixture of **1** [28,29] (0.47 g, 2 mmol) and hydrazine hydrate 80% (0.2 mL) in ethanol (5 mL) was heated under reflux for 5 h. The reaction mixture was cooled to room temperature and the obtained precipitate was filtered, washed with ethanol, dried and crystallized from ethanol. White crystals (0.38 g, 83%); mp 132–134 °C; IR (KBr, $cm^{-1}$): 3421, 3309, 3287 (NH, $NH_2$), 1591, 1492 (C=O, C=C Ar); $^1H$ NMR (300 MHz, $\delta$ ppm): 4.33 (s, 2H, NH*$NH_2$*, $D_2O$ exchangeable), 6.19 (s, 2H, thiophene $NH_2$, $D_2O$ exchangeable), 7.34–7.49 (m, 6H, 5Ar-H and thiophene-$C^5$-H), 7.56 (s, br, 1H, *NH*$NH_2$, $D_2O$ exchangeable); $^{13}C$ NMR (75 MHz, $\delta$ ppm): 101.9, 126.0, 127.9, 128.3, 129.3, 133.6, 135.1, 150.7, 165.8; Anal. Calcd for $C_{11}H_{11}N_3OS$ (233.29): C, 56.63; H, 4.75; N, 18.01. Found: C, 56.84; H, 4.82; N, 18.23.

#### 4.1.2. Ethyl 1-(3-amino-4-phenylthiophene-2-carbonyl)-5-hydroxy-1H-pyrazole-4-carboxylate (3)

A mixture of **2** (0.47 g, 2 mmol), diethyl ethoxymethylenemalonate (0.43 g, 0.4 mL, 2 mmol) and anhydrous potassium carbonate (0.28 g, 2 mmol) in absolute ethanol (5 mL) was heated under reflux for 6 h. After being cooled to room temperature, the produced solid was filtered, suspended in water, neutralized with 10% hydrochloric acid. The obtained precipitate was filtered, washed with water, dried and crystallized from ethanol. White crystals (0.58 g, 81%); mp 280–282 °C; IR (KBr, $cm^{-1}$): 3483, 3436, 3345 (OH, $NH_2$), 1693 (C=O ester), 1630 (C=O), 1580, 1532 (C=N, C=C Ar), 1365, 1179 ($\upsilon_{as}$ and $\upsilon_s$ C–O–C); $^1H$ NMR (300 MHz, $\delta$ ppm): 1.18 (t, $J$ = 7.2 Hz, 3H, $CH_2CH_3$), 4.02 (q, $J$ = 7.2 Hz, 2H, $CH_2CH_3$), 6.82 (s, 2H, $NH_2$, $D_2O$ exchangeable), 7.36–7.51 (m, 5H, Ar-H), 7.53 (s, 1H, thiophene-$C^5$-H), 7.58 (s, 1H, pyrazole-$C^3$-H); $^{13}C$ NMR (75 MHz, $\delta$ ppm): 15.3, 56.5, 90.1, 101.2, 127.8, 128.4, 129.4, 131.6, 134.8, 135.1, 144.0, 155.2, 163.6, 164.5, 165.7; EI-MS $m/z$ (%): 357 ($M^{+\cdot}$) (23), 294 (100); Anal. Calcd for $C_{17}H_{15}N_3O_4S$ (357.38): C, 57.13; H, 4.23; N, 11.76; S, 8.97. Found: C, 57.39; H, 4.27; N, 11.89; S, 9.03.

#### 4.1.3. Ethyl 3-(2-(3-amino-4-phenylthiophene-2-carbonyl)hydrazinyl)-2-cyanoprop-2-enoate (4)

A mixture of **2** (0.47 g, 2 mmol), ethyl ethoxymethylenecyanoacetate (0.34 g, 2 mmol) and anhydrous potassium carbonate (0.28 g, 2 mmol) in absolute ethanol (5 mL) was heated under reflux for 6 h. After being cooled to room temperature, the solid product was filtered, washed with water, dried and crystallized from dioxane. White crystals (0.51 g, 71%); mp 292–294 °C; IR (KBr, $cm^{-1}$): 3443 (br, NH, $NH_2$), 2195 (C≡N), 1675 (ester C=O), 1643 (C=O), 1542 (C=C Ar), 1280, 1111 ($\upsilon_{as}$ and $\upsilon_s$ C–O–C); $^1H$ NMR (300 MHz, $\delta$ ppm): 1.15 (t, $J$ = 7.2 Hz, 3H, $CH_2CH_3$), 3.98 (q, $J$ = 7.2 Hz, 2H, $CH_2CH_3$), 7.37–7.50 (m, 3H, phenyl-$C^{3,4,5}$-H), 7.97–8.0 (m, 2H, phenyl-$C^{2,6}$-H), 8.25 (s, 2H, $NH_2$, $D_2O$ exchangeable), 8.34 (s, 1H, thiophene-$C^5$-H), 8.37 (s, 1H, =CH); $^{13}C$ NMR (75 MHz, $\delta$ ppm): 15.4, 58.2, 121.6, 124.7, 128.1, 128.4, 128.9, 131.0, 134.1, 136.6, 147.8, 153.2, 155.8, 168.5, 169.1; HRMS calculated $[M+H]^{+\cdot}$ For $C_{17}H_{17}N_4O_3S$: 357.102, found: 357.099; Anal. Calcd for $C_{17}H_{16}N_4O_3S$ (356.40): C, 57.29; H, 4.52; N, 15.72; S, 9.00. Found: C, 57.54; H, 4.29; N, 15.98; S, 9.12.

#### 4.1.4. 1-(3-Amino-4-phenylthiophen-2-yl)carbonyl-3,5-dimethyl-1H-pyrazole (5)

Acetylacetone (0.3 g, 0.31 mL, 3 mmol) was added to a solution of **2** (0.47 g, 2 mmol) in absolute ethanol (5 mL) and the reaction mixture was heated under reflux for 10 h. The reaction mixture was concentrated and left to cool to room temperature. The obtained precipitate was filtered, dried and crystallized from ethanol. White crystals (0.33 g, 55%); mp 140–142 °C; IR (KBr, $cm^{-1}$): 3456, 3339 ($NH_2$), 1639 (C=O), 1590, 1536 (C=N, C=C Ar); $^1H$ NMR (300 MHz, $\delta$ ppm): 2.24 (s, 3H, $CH_3$), 2.51 (s, 3H, $CH_3$), 6.20 (s, 1H, pyrazole-$C^4$-H), 7.13 (s, 2H, $NH_2$, $D_2O$ exchangeable), 7.40–7.49 (m, 5H, Ar-H), 7.80 (s, 1H, thiophene-$C^5$-H);$^{13}C$ NMR (100 MHz, $\delta$ ppm): 14.0, 14.7, 99.6, 111.0, 128.1, 128.5, 129.5, 131.6, 134.4, 137.5, 143.9, 150.4, 157.3, 163.1; Anal. Calcd for $C_{16}H_{15}N_3OS$ (297.37): C, 64.62; H, 5.08; N, 14.13; S, 10.78. Found: C, 64.73; H, 5.12; N, 14.28; S, 10.86.

#### 4.1.5. General procedure for the synthesis of 3-amino-4-phenyl-N′-((1-phenyl-3-(4-substituted phenyl)-1H-pyrazol-4-yl)methylene)thiophene-2-carbohydrazides (6a-c)

To a suspension of **2** (0.47 g, 2 mmol) in ethanol (5 mL), the appropriate pyrazole-4-carboxaldehyde (2 mmol) was added. The reaction mixture was heated under reflux for 12 h then allowed to cool to room temperature. The obtained precipitate was filtered, washed with ethanol, dried and crystallized from dioxane/ethanol.

*4.1.5.1. 3-Amino-4-phenyl-N′-((1,3-diphenyl-1H-pyrazol-4-yl)methylene) thiophene-2-carbohydrazide (6a).* Pale yellow crystals (0.73 g, 78%); mp 245–247 °C; IR (KBr, $cm^{-1}$): 3454, 3429, 3323 (NH, $NH_2$), 1627 (C=O), 1591, 1504 (C=N, C=C Ar); $^1H$ NMR (400 MHz, $\delta$ ppm): 6.71 (br s, 2H, $NH_2$, $D_2O$ exchangeable), 7.37–7.60 (m, 12H, 11Ar-H, thiophene-$C^5$-H),7.64 (s, 1H, pyrazole-$C^5$-H), 7.72 (d, $J$ = 7.04 Hz, 2H, pyrazole-

$C^3$-phenyl-$C^{2,6}$-H), 8.00 (d, $J$ = 7.8 Hz, 2H, pyrazole-*N*-phenyl-$C^{2,6}$-H), 8.25, 8.80 (2 s, 1H, =CH, Z and E isomers), 11.19 (s, 1H, NH, $D_2O$ exchangeable); EI-MS *m/z* (%): 463 ($M^{+\bullet}$) (100); Anal. Calcd for $C_{27}H_{21}N_5OS$ (463.55): C, 69.96; H, 4.57; N, 15.11; S, 6.92. Found: C, 70.14; H, 4.63; N, 15.24; S, 6.99.

*4.1.5.2. 3-Amino-N′-((3-(4-chlorophenyl)-1-phenyl-1H-pyrazol-4-yl) methylene)-4-phenylthiophene-2-carbohydrazide* ***(6b)***. White crystals (0.92 g, 92%); mp 276–278 °C; IR (KBr, $cm^{-1}$): 3460, 3433, 3320 (NH, $NH_2$), 1627 (C=O), 1579, 1503 (C=N, C=C Ar); $^1$H NMR (500 MHz, $\delta$ ppm): 6.68 (s, br, 2H, $NH_2$, $D_2O$ exchangeable), 7.34–7.58 (m, 12H, 10Ar-H, thiophene-$C^5$-H and pyrazole-$C^5$-H), 7.71 (d, $J$ = 7.75 Hz, 2H, 4-chlorophenyl-$C^{3,5}$-H), 7.94 (d, $J$ = 7.75 Hz, 2H, 4-chlorophenyl-$C^{2,6}$-H), 8.16, 8.77 (2 s, 1H, =CH, Z and E isomers), 11.17 (s, 1H, NH, $D_2O$ exchangeable); $^{13}$C NMR (125 MHz, $\delta$ ppm): 117.8, 119.6, 127.4, 127.7, 127.9, 128.4, 129.3, 129.4, 130.2, 130.5, 131.1, 131.5, 133.8, 133.9, 135.0, 138.6, 139.4, 139.8, 143.5, 150.7, 160.0; Anal. Calcd for $C_{27}H_{20}ClN_5OS$ (498.00): C, 65.12; H, 4.05; N, 14.06; S, 6.44. Found: C, 65.27; H, 4.11; N, 14.17; S, 6.48.

*4.1.5.3. 3-Amino-N′-((3-(4-methylphenyl)-1-phenyl-1H-pyrazol-4-yl) methylene)-4-phenylthiophene-2-carbohydrazide* ***(6c)***. White crystals (0.86 g, 90%); mp 258–260 °C; IR (KBr, $cm^{-1}$): 3482, 3468, 3332 (NH, $NH_2$), 1629 (C=O), 1594, 1505 (C=N, C=C Ar); $^1$H NMR (400 MHz, $\delta$ ppm): 2.40 (s, 3H, $CH_3$), 6.71 (br s, 2H, $NH_2$, $D_2O$ exchangeable), 7.35–7.62 (m, 13H, 12Ar-H, thiophene-$C^5$-H),7.64 (s, 1H, pyrazole-$C^5$-H), 7.98 (d, $J$ = 7.8 Hz, 2H, 4-methylphenyl-$C^{2,6}$-H), 8.23, 8.78 (2 s, 1H, =CH, Z and E isomers), 11.18 (s, 1H, NH, $D_2O$ exchangeable); $^{13}$C NMR (100 MHz, $\delta$ ppm): 21.4, 117.6, 119.5, 126.9, 127.5, 127.9, 128.4, 128.6, 128.7, 129.4, 129.7 (2C), 129.9, 130.0, 130.1, 135.0 (2C), 136.0, 138.5, 139.6, 143.4, 152.1, 165.1; EI-MS *m/z* (%): 477 ($M^{+\bullet}$) (5), 365 (100); Anal. Calcd for $C_{28}H_{23}N_5OS$ (477.58): C, 70.42; H, 4.85; N, 14.66; S, 6.71. Found: C, 70.61; H, 4.89; N, 14.83; S, 6.82.

*4.1.6. 4-Hydrazino-7-phenylthieno[3,2-d]pyrimidine* ***(8)***

A mixture of **7** [31](0.49 g, 2 mmol) in hydrazine hydrate 99% (2 mL) was heated under reflux for 1 h. The reaction mixture was cooled to room temperature and poured onto ice/cold water. The obtained precipitate was filtered, washed with ethanol, dried and crystallized from ethanol. Brown crystals (0.34 g, 71%); mp 176–178 °C; IR (KBr, $cm^{-1}$): 3448, 3333, 3194 (NH, $NH_2$), 1651 (C=N), 1567, 1463 (C=C Ar);$^1$H NMR (500 MHz, $\delta$ ppm): 4.86 (s, 2H, $NH_2$, $D_2O$ exchangeable), 7.31–8.03 (m, 5H, Ar-H), 8.27 (s, 1H, thienopyrimidine-$C^6$-H), 8.28 (s, 1H, thienopyrimidine-$C^2$-H), 9.03 (s, 1H, NH, $D_2O$ exchangeable); Anal. Calcd for $C_{12}H_{10}N_4S$ (242.30): C, 59.48; H, 4.16; N, 23.12. Found: C, 59.54; H, 3.92; N, 22.88.

*4.1.7. 5-Amino-1-(7-phenylthieno[3,2-d]pyrimidin-4-yl)-1H-pyrazole-4-carbonitrile* ***(9)***

A mixture of **8** (0.48 g, 2 mmol), ethoxymethylenemalononitrile (0.24 g, 2 mmol) and anhydrous potassium carbonate (0.28 g, 2 mmol) in absolute ethanol (5 mL) was heated under reflux for 6 h. After being cooled to room temperature, the produced solid was separated, washed with water, dried and crystallized from ethanol. White crystals (0.50 g, 79%); mp 290–292 °C; IR (KBr, $cm^{-1}$): 3381, 3286 ($NH_2$), 2224 (CN), 1636 (C=N), 1554, 1480 (C=C Ar); $^1$H NMR (300 MHz, $\delta$ ppm): 7.41–7.49 (m, 3H, phenyl-$C^{3,4,5}$-H), 8.04–8.07 (m, 2H, phenyl-$C^{2,6}$-H), 8.18 (s, 1H, thienopyrimidine-$C^6$-H), 8.58 (s, br, 2H, $NH_2$, $D_2O$ exchangeable), 8.76 (s, 1H, pyrazole-$C^3$-H), 9.10 (s, 1H, thienopyrimidine-$C^2$-H), $^{13}$C NMR (75 MHz, $\delta$ ppm): 73.4, 113.7, 118.1, 127.6, 128.0, 128.2, 132.9, 134.7, 137.8, 143.9, 152.1, 153.5, 154.1, 159.5; EI-MS *m/z* (%): 318 ($M^{+\bullet}$) (100); Anal. Calcd for $C_{16}H_{10}N_6S$ (318.36): C, 60.36; H, 3.17; N, 26.40; S, 10.07. Found: C, 60.62; H, 3.14; N, 26.70; S, 10.34.

*4.1.8. Ethyl 5-amino-1-(7-phenylthieno[3,2-d]pyrimidin-4-yl)-1H-pyrazole-4-carboxylate* ***(10)***

A mixture of **8** (0.48 g, 2 mmol), ethyl ethoxymethylenecyanoacetate (0.34 g, 2 mmol) and anhydrous potassium carbonate (0.28 g, 2 mmol) in absolute ethanol (5 mL) was heated under reflux for 6 h. After being cooled to room temperature, the produced solid was separated, washed with water, dried and crystallized from ethanol. White crystals (0.53 g, 74%); mp 179–181 °C; IR (KBr, $cm^{-1}$): 3445, 3332 ($NH_2$), 1686 (C=O ester), 1617 (C=N), 1556, 1483 (C=C Ar), 1301, 1129 ($\upsilon_{as}$ and $\upsilon_s$ C−O−C); $^1$H NMR (300 MHz, $\delta$ ppm): 1.31 (t, $J$ = 7.2 Hz, 3H, $CH_2CH_3$), 4.27 (q, $J$ = 7.2 Hz, 2H, $CH_2CH_3$), 7.41–7.54 (m, 3H, phenyl-$C^{3,4,5}$-H), 7.99 (s, br, 2H, $NH_2$, $D_2O$ exchangeable), 8.03 (s, 1H, thienopyrimidine-$C^6$-H), 8.04–8.08 (m, 2H, phenyl-$C^{2,6}$-H), 8.75 (s, 1H, pyrazole-$C^3$-H), 9.10 (s, 1H, thienopyrimidine-$C^2$-H); $^{13}$C NMR (75 MHz, $\delta$ ppm): 19.0, 56.5, 94.9, 118.9, 128.4, 128.7, 129.0, 133.6, 135.4, 138.6, 143.4, 153.0, 153.2, 154.5, 160.2, 163.4; EI-MS *m/z* (%): 365 ($M^{+\bullet}$) (100); Anal. Calcd for $C_{18}H_{15}N_5O_2S$ (365.41): C, 59.16; H, 4.14; N, 19.17. Found: C, 59.13; H, 3.93; N, 18.90.

*4.1.9. Ethyl 5-hydroxy-1-(7-phenylthieno[3,2-d]pyrimidin-4-yl)-1H-pyrazole-4-carboxylate* ***(11)***

An equimolar mixture of **8** (0.48 g, 2 mmol), diethyl ethoxymethylenemalonate (0.45 g, 2 mmol) and anhydrous potassium carbonate (0.28 g, 2 mmol) in ethanol (5 mL) was heated under reflux for 12 h. The separated solid product was suspended in water, neutralized with 10% hydrochloric acid. The obtained precipitate was filtered, dried and crystallized from ethanol. Yellow crystals (0.61 g, 84%); mp: 290–292 °C; IR (KBr, $cm^{-1}$): 3429 (br, OH), 1710 (C=O), 1627, 1516 (C=N, C=C Ar), 1317, 1141 ($\upsilon_{as}$ and $\upsilon_s$ C−O−C); $^1$H NMR (300 MHz, $\delta$ ppm): 1.28 (t, $J$ = 7.2 Hz, 3H, $CH_2CH_3$), 4.23 (q, $J$ = 7.2 Hz, 2H, $CH_2CH_3$), 7.43–7.55 (m, 3H, phenyl-$C^{3,4,5}$-H), 8.02–8.06 (m, 2H, phenyl-$C^{2,6}$-H), 8.16 (s, 1H, thienopyrimidine-$C^6$-H), 8.87 (s, 1H, pyrazole-$C^3$-H), 9.11 (s, 1H, thienopyrimidine-$C^2$-H); $^{13}$C NMR (100 MHz, $\delta$ ppm): 18.9, 56.4, 112.0, 112.2, 118.2, 128.6, 128.8, 129.0, 133.3, 135.6, 139.8, 145.6, 151.0, 152.8, 160.2, 160.3; EI-MS *m/z* (%): 366 ($M^{+\bullet}$) (75), 320 (100); Anal. Calcd for $C_{18}H_{14}N_4O_3S$ (366.39): C, 59.01; H, 3.85; N, 15.29. Found: C, 59.23; H, 3.91; N, 15.41.

*4.1.10. 4-(3,5-Dimethyl-1H-pyrazol-1-yl)-7-phenylthieno[3,2-d] pyrimidine* ***(12)***

A solution of **8** (0.48 g, 2 mmol) in absolute ethanol (5 mL) was treated with acetylacetone (0.3 g, 0.31 mL, 3 mmol) and the reaction mixture was heated under reflux for 10 h. The reaction mixture was concentrated and left to cool to room temperature. The obtained precipitate was filtered, washed with ethanol, dried and crystallized from ethanol. White crystals (0.2 g, 33%); mp 139–141 °C; IR (KBr, $cm^{-1}$): 1627 (C=N), 1580, 1481 (C=C Ar);$^1$H NMR (300 MHz, $\delta$ ppm): 2.31 (s, 3H, $CH_3$), 2.78 (s, 3H, $CH_3$), 6.31 (s, 1H, pyrazole-$C^4$-H), 7.40–7.52 (m, 3H, phenyl-$C^{3,4,5}$-H), 8.05–8.08 (m, 2H, phenyl-$C^{2,6}$-H), 8.67 (s, 1H, thienopyrimidine-$C^6$-H), 9.04 (s, 1H, thienopyrimidine-$C^2$-H); Anal. Calcd for $C_{17}H_{14}N_4S$ (306.38): C, 66.64; H, 4.61; N, 18.29; S, 10.47. Found: C, 66.79; H, 4.69; N, 18.41; S, 10.54.

*4.1.11. 4-(2-((3-(4-Chlorophenyl)-1-phenyl-1H-pyrazol-4-yl)methylene) hydrazinyl)-7-phenylthieno[3,2-d]pyrimidine* ***(13)***

To a suspension of **8** (0.48 g, 2 mmol) in ethanol (5 mL), 3-(4-chlorophenyl)-1-phenyl-1*H*-pyrazole-4-carboxaldehyde (0.57, 2 mmol) was added. The reaction mixture was heated under reflux for 6 h then allowed to cool. The obtained precipitate was filtered, washed with ethanol, dried and crystallized from dioxane. White crystals (0.90 g, 90%); mp > 300 °C; IR (KBr, $cm^{-1}$): 3445 (NH), 1596, 1501 (C=N, C=C Ar); $^1$H NMR (300 MHz, $\delta$ ppm): 7.37–7.79 (m, 10H, Ar-H), 8.02 (d, $J$ = 8.2 Hz, 2H, 4-chlorophenyl-$C^{2,6}$-H), 8.08 (d, $J$ = 8.2 Hz, 2H, 4-chlorophenyl-$C^{3,5}$-H), 8.35 (s, 1H, thienopyrimidine-$C^6$-H), 8.46 (s, 1H, pyrazole-$C^5$-H), 8.61 (s, 1H, =CH), 8.86 (s, 1H, thienopyrimidine-$C^2$-

H), 11.97 (s, 1H, NH, $D_2O$ exchangeable); $^{13}C$ NMR (100 MHz, $\delta$ ppm): 114.0, 119.7, 120.8, 124.4, 127.2, 127.8, 128.6, 128.8, 129.3, 129.4, 130.1, 130.4, 130.5, 131.4, 131.5, 133.9, 135.6, 139.5, 142.2, 143.9, 153.1, 157.0; Anal. Calcd for $C_{28}H_{19}ClN_6S$ (507.01): C, 66.33; H, 3.78; N, 16.58; S, 6.32. Found: C, 66.47; H, 3.84; N, 16.67; S, 6.43.

*4.1.12. 8-Bromo-3-(3-(4-chlorophenyl)-1-phenyl-1H-pyrazol-4-yl)-7-phenylthieno[2,3-e][1,2,4]triazolo[4,3-c]pyrimidine (**14**)*

A mixture of **13** (0.51 g, 1 mmol) and anhydrous sodium acetate (0.25 g, 3 mmol) in glacial acetic acid (3 mL) was treated with bromine (0.32 g, 0.1 mL, 2 mmol) and the reaction mixture was stirred at room temperature for an overnight then poured onto ice/cold water. The obtained precipitate was filtered, washed with water, dried and crystallized from dioxane. White crystals (0.56 g, 95%); mp: 254–256 °C; IR (KBr, $cm^{-1}$): 1630 (C═N), 1575, 1499 (C═C Ar); $^1H$ NMR (300 MHz, $\delta$ ppm): 7.48–7.74 (m, 10*H*, Ar-H), 7.95 (d, $J$ = 8.7 Hz, 2H, 4-chlorophenyl-$C^{2,6}$-H), 8.02 (d, $J$ = 8.7 Hz, 2H, 4-chlorophenyl-$C^{3,5}$-H), 9.33 (s, 1H, pyrazole-$C^5$-H), 9.61 (s, 1H, thienotriazolopyrimidine-$C^5$-H); $^{13}C$ NMR (100 MHz, $\delta$ ppm): 85.3, 103.8, 119.3, 119.7, 128.5, 128.6, 128.8, 128.9, 129.0, 129.4, 130.1, 130.2, 130.5, 130.7, 131.2, 133.9, 135.1, 141.5, 147.1, 151.0, 154.4, 157.0; EI-MS $m/z$ (%): 586 ($M^{+\bullet}$+4) (21), 584 ($M^{+\bullet}$+2) (68), 582 ($M^{+\bullet}$) (48), 63 (100); Anal. Calcd for $C_{28}H_{16}BrClN_6S$ (583.89): C, 57.60; H, 2.76; N, 14.39. Found: C, 57.89; H, 2.79; N, 14.62.

*4.2. Biological activity*

*4.2.1. In vitro COX-1 and COX-2 enzymatic inhibition assay [33]*

The inhibitory COX activity of the newly synthesized compounds in addition to celecoxib and indomethacin were assayed according to the instructions of the use of Cayman colorimetric COX (ovine) inhibitor screening assay kit (Catalog No. 760111, Cayman chemicals, MI, USA). The concentration causing 50% enzyme inhibition ($IC_{50}$, μM) was determined. In addition, COX-1/COX-2 selectivity ratios of the test compounds were estimated.

*4.2.2. In vivo anti-inflammatory activity*

Male albino rats weighing 180–200 g were used to study the anti-inflammatory, ulcerogenic liability and acute toxicity. Animals (five per cage) were housed under controlled laboratory conditions and were allowed standard chow and water *ad libitum*. All experimental procedures involving animals were performed in strict accordance with The Institutional Animal Care and Use Committee ethical standards. Experimental protocol was approved by Institutional Animal Care and Use Committee, Faculty of Medicine, Alexandria University, Alexandria, Egypt (AlexU-IACUC code: 0634).

*4.2.2.1. Formalin-induced paw edema bioassay (acute inflammatory model)*. The acute anti-inflammatory activity for the newly synthesized compounds and the reference drugs diclofenac sodium and celecoxib were evaluated using formalin-induced paw edema bioassay and the measurement of paw volume (mL) was done at zero time and after 1 h, 2 h and 4 h of administration of formalin according to the reported method [30,34]. The edema was expressed as an increase in the paw volume and the percentage of edema inhibition (EI%) was obtained as follows:

$$EI\% = (V_t - V_0)_{control} - (V_t - V_0)_{test\ compound}/(V_t - V_0)_{control} \times 100$$

where $V_t$ = volume of edema at specific time interval and $V_0$ = volume of edema at zero time interval.

*4.2.2.2. Formalin-induced paw edema bioassay (sub-acute inflammatory model)*. Sub-acute anti-inflammatory activities of all test compounds were conducted on the rats of the first experiment and the changes in the volume of paw were measured plethymographically at day 1 and day 8 according to the reported method [34,35].

*4.2.2.3. Determination of effective dose 50 ($ED_{50}$) [30]*. Compounds **3**, **6a**, **6c**, **9**, **10** and **11** that showed promising *in vivo* anti-inflammatory activities and the references diclofenac sodium and celecoxib were further tested at 5, 10, 20, 40, and 50 mg/kg body weight and the $ED_{50}$ was determined by measuring the inhibition of the edema volume 2 h after formalin injection according to the reported method [30].

*4.2.2.4. Determination of ulcerogenic activity*. Compounds **3**, **6a**, **6c**, **9**, **10** and **11** that exhibited pronounced *in vivo* anti-inflammatory profiles were further evaluated for their ulcerogenic potential in male albino rats according to the reported method using diclofenac sodium, indomethacin and celecoxib as reference standards [36]. Test compounds were given at 0 and 12 h for three successive days at a dose of 300 mg/kg per day. Animals were sacrificed and their stomachs were inspected for any evidence of hyperemia, hemorrhage, definite hemorrhagic erosion or ulcer.

*4.2.2.5. Determination of acute toxicity*. The most active compounds (**3**, **6a**, **6c**, **9**, **10** and **11**) were further evaluated for their approximate acute lethal dose ($ALD_{50}$) using a literature method [30,37]. The compounds were given orally in graded doses of 100–400 mg/kg body weight, screened for their acute lethal doses ($ALD_{50}$) and mortalities were recorded at each dose level after 24 h.

*4.2.3. In silico studies*

*4.2.3.1. Docking studies*. Docking studies were performed using Molecular Operating Environment (MOE) version 2014.09 [38] running on an Intel Core i5PC running Windows 10 as operating system. Crystal structure of COX-2 complexed with celecoxib (PDB code 3LN1) [39] was retrieved from the Protein Data Bank. 3D structures for compounds **3, 6a, 6c, 9, 10, 11** and **13** were constructed using the Builder module of MOE and optimized by energy minimization using MMFF94X forcefield. All docking calculations were carried out using the MOE Dock module. The parameters used were alpha triangle as placement methodology and London dG as scoring function with forcefield refinement. Ligand interactions were generated using the Ligand Interactions module in MOE. The docking protocol was validated by docking celecoxib in the active site of 3LN1, where the docked celecoxib showed 0.4 Å Root Mean Square Distance (RMSD) from the co-crystallized celecoxib.

*4.2.3.2. Chemo-informatic properties evaluation*. ADME properties of compounds **3, 6a, 6c, 9, 10, 11** and **13** were obtained computationally through Molinspiration tool [41] (http://www.molinspiration.com/cgi-bin/properties) where numbers of hydrogen donors (*n*-OHNH) and acceptors (*n*-ON), c log*P* and total polar surface area (TPSA) in addition to violations from Lipinski's RO5 were calculated. Moreover, % absorption (% ABS) was calculated from the following equation: % ABS = 109–0.345 TPSA [44]. The aqueous solubility (Mol log S in mg/L**)** and the drug likeness model score of the most active compounds were predicted using Molsoft software (http://molsoft.com/mprop/) [43,45]. Furthermore, the predicted human intestinal absorption (HIA), blood–brain barrier penetration (BBB) and plasma protein binding (PPB) (ADME properties) were evaluated by Pre ADMET calculator [46] to evaluate the overall pharmacokinetic profiles of the compounds.

## Conflicts of interest

The authors have no conflict of interest to declare.

## Funding

This research did not receive any specific grant from funding agencies in the public, commercial, or not-for-profit sectors.

## References


[1] M. Ahmed, M. Abdul Qadir, A. Hameed, M. Imran, M. Muddassar, Screening of curcumin-derived isoxazole, pyrazoles and pyrimidines for their anti-inflammatory, antinociceptive and cyclooxygenase-2 inhibition, Chem. Biol. Drug Des. 91 (2018) 338–343, https://doi.org/10.1111/cbdd.13076.

[2] C. Dayakar, B.S. Kumar, G. Sneha, G. Sagarika, K. Meghana, S. Ramakrishna, R.S. Prakasham, B. China Raju, Synthesis, pharmacological activities and molecular docking studies of pyrazolyltriazoles as anti-bacterial and anti-inflammatory agents, Bioorg. Med. Chem. 25 (2017) 5678–5691, https://doi.org/10.1016/j.bmc.2017.08.042.

[3] M.A. Abdelgawad, M.B. Labib, W.A.M. Ali, G. Kamel, A.A. Azouz, E.S. EL-Nahass, Design, synthesis, analgesic, anti-inflammatory activity of novel pyrazolones possessing aminosulfonyl pharmacophore as inhibitors of COX-2/5-LOX enzymes: Histopathological and docking studies, Bioorg. Chem. 78 (2018) 103–114, https://doi.org/10.1016/j.bioorg.2018.03.011.

[4] J.V. Faria, P.F. Vegi, A.G.C. Miguita, M.S. dos Santos, N. Boechat, A.M.R. Bernardino, Recently reported biological activities of pyrazole compounds, Bioorg. Med. Chem. 25 (2017) 5891–5903, https://doi.org/10.1016/j.bmc.2017.09.035.

[5] L.S. Pavase, D.V. Mane, K.G. Baheti, Anti-inflammatory exploration of sulfonamide containing diarylpyrazoles with promising COX-2 selectivity and enhanced gastric safety profile, J. Het. Chem. 55 (2018) 913–922, https://doi.org/10.1002/jhet.3118.

[6] N. Chandna, J.K. Kapoor, J. Grover, K. Bairwa, V. Goyal, S.M. Jachak, Pyrazolylbenzyltriazoles as cyclooxygenase inhibitors: synthesis and biological evaluation as dual anti-inflammatory and antimicrobial agents, New J. Chem. 38 (2014) 3662–3672, https://doi.org/10.1039/C4NJ00226A.

[7] K.R.A. Abdellatif, W.A.A. Fadaly, New 1,2-diaryl-4-substituted-benzylidene-5-4*H*-imidazolone derivatives: design, synthesis and biological evaluation as potential anti-inflammatory and analgesic agents, Bioorg. Chem. 72 (2017) 123–129, https://doi.org/10.1016/j.bioorg.2017.04.002.

[8] M.T. El Sayed, M.A.M.S. El-Sharief, E.S. Zarie, N.M. Morsy, A.R. Elsheakh, A. Voronkov, V. Berishvili, G.S. Hassan, Design, synthesis, anti-inflammatory activity and molecular docking of potential novel antipyrine and pyrazolone analogs as cyclooxygenase enzyme (COX) inhibitors, Bioorganic Med. Chem. Lett. 28 (2018) 952–957, https://doi.org/10.1016/j.bmcl.2018.01.043.

[9] M.A. Abdelgawad, M.B. Labib, M. Abdel-Latif, Pyrazole-hydrazone derivatives as anti-inflammatory agents: design, synthesis, biological evaluation, COX-1,2/5-LOX inhibition and docking study, Bioorg. Chem. 74 (2017) 212–220, https://doi.org/10.1016/j.bioorg.2017.08.014.

[10] K.R.A. Abdellatif, M.A. Abdelgawad, M.B. Labib, T.H. Zidan, Synthesis and biological evaluation of new diarylpyrazole and triarylimidazoline derivatives as selective COX-2 Inhibitors, Arch. Pharm. Chem. Life Sci. 350 (2017) e1600386, https://doi.org/10.1002/ardp.201600386.

[11] N. Inceler, Y. Ozkan, N.N. Turan, D.C. Kahraman, R. Cetin-Atalay, S.N. Baytas, Design, synthesis and biological evaluation of novel 1,3-diarylpyrazoles as cyclooxygenase inhibitors, antiplatelet and anticancer agents, MedChemComm 9 (2018) 795–811, https://doi.org/10.1039/C8MD00022k.

[12] M.B. Labib, S.M.Z. Sharkawi, M. El-Daly, Design, synthesis of novel isoindoline hybrids as COX-2 inhibitors: anti-inflammatory, analgesic activities and docking study, Bioorg. Chem. 80 (2018) 70–80, https://doi.org/10.1016/j.bioorg.2018.05.018.

[13] G. Carullo, F. Galligano, F. Aiello, Structure–activity relationships for the synthesis of selective cyclooxygenase 2 inhibitors: an overview (2009–2016), MedChem Comm. 8 (2017) 492–500, https://doi.org/10.1039/c6md00569a.

[14] S.S.R. Alsayed, H.A.H. Elshemy, M.A. Abdelgawad, M.S. Abdel-Latif, K.R.A. Abdellatif, Design, synthesis and biological screening of some novel celecoxib and etoricoxib analogs with promising COX-2 selectivity, anti-inflammatory activity and gastric safety profile, Bioorg. Chem. 70 (2017) 173–183, https://doi.org/10.1016/j.bioorg.2016.12.008.

[15] D. Korobko, D.J. Hadjipavlou-litina, L. Logoyda, Antioxidant and anti-inflammatory properties of a series of new 7,8-disubstituted theophylline containing a pyrazole ring, Asian J. Pharm. Clin. Res. 11 (2018) 448–450 https://doi.org/10.22159/ajpcr.2018.v11i6.25990.

[16] M.G. Prabhudeva, S. Bharath, A.D. Kumar, S. Naveen, N.K. Lokanath, B.N. Mylarappa, K.A. Kumar, Design and environmentally benign synthesis of novel thiophene appended pyrazole analogues as anti-inflammatory and radical scavenging agents: Crystallographic, *in silico* modeling, docking and SAR characterization, Bioorg. Chem. 73 (2017) 109–120, https://doi.org/10.1016/j.bioorg.2017.06.004.

[17] K.R.A. Abdellatif, E.K.A. Abdelall, W.A.A. Fadaly, G.M. Kamel, Synthesis, cyclooxygenase inhibition, anti-inflammatory evaluation and ulcerogenic liability of new 1,3,5-triarylpyrazoline and 1,5-diarylpyrazole derivatives as selective COX-2 inhibitors, Bioorganic Med. Chem. Lett. 26 (2016) 406–412, https://doi.org/10.1016/j.bmcl.2015.11.105.

[18] G.N. Tageldin, S.M. Fahmy, H.M. Ashour, M.A. Khalil, R.A. Nassra, I.M. Labouta, Design, synthesis and evaluation of some pyrazolo[3,4-d]pyrimidines as anti-inflammatory agents, Bioorg. Chem. 78 (2018) 358–371, https://doi.org/10.1016/j.bioorg.2018.03.030.

[19] M.N. Kumbar, R.R. Kamble, J.P. Dasappa, P.K. Bayannavar, H.A. Khamees, M. Mahendra, S.D. Joshi, S. Dodamani, V.P. Rasal, S. Jalalpure, 5-(1-Aryl-3-(thiophen-2-yl)-1*H*-pyrazol-4-yl)-1*H*-tetrazoles: Synthesis, structural characterization, Hirshfeld analysis, anti-inflammatory and anti-bacterial studies, J. Mol. Struct. 1160 (2018) 63–72, https://doi.org/10.1016/j.molstruc.2018.01.047.

[20] K.A.K. Musa, L.A. Eriksson, Photodegradation mechanism of non steroidal anti-inflammatory drugs containing thiophene moieties: suprofen and tiaprofenic acid, J. Phys. Chem. B 113 (2009) 11306–11313 https://pubs.acs.org/doi/abs/10.1021/jp904171p.

[21] F.A. Ragab, H.I. Heiba, M.G. El-Gazzar, S.M. Abou-Seri, W.A. El-Sabbagh, R.M. El-Hazek, Anti-inflammatory, analgesic and COX-2 inhibitory activity of novel thiadiazoles in irradiated rats, J. Photochem. Photobiol. B 166 (2017) 285–300, https://doi.org/10.1016/j.jphotobiol.2016.12.007.

[22] A.A. Bekhit, A.M. Farghaly, R.M. Shafik, M.M.A. Elsemary, A.E.-D.A. Bekhit, A.A. Guemei, M.S. El-Shoukrofy, T.M. Ibrahim, Synthesis, biological evaluation and molecular modeling of novel thienopyrimidinone and triazolothienopyrimidinone derivatives as dual anti-inflammatory antimicrobial agents, Bioorg. Chem. 77 (2018) 38–46, https://doi.org/10.1016/j.bioorg.2017.12.028.

[23] M.S. Tolba, M. Ahmed, A.M. Kamal El-Dean, R. Hassanien, M. Farouk, Synthesis of new fused thienopyrimidines derivatives as anti-inflammatory agents, J. Het. Chem. 55 (2018) 408–418, https://doi.org/10.1002/jhet.3056.

[24] A.A. Bekhit, A.M. Farghaly, R.M. Shafik, M.M. Elsemary, M.S. El-Shoukrofy, A.E.-D.A. Bekhit, T.M. Ibrahim, Synthesis, evaluation and modeling of some triazolothienopyrimidinones as anti-inflammatory and antimicrobial agents, Future Med. Chem. 9 (2017) 881–897, https://doi.org/10.4155/fmc-2016-0242.

[25] O.M. AboulWafa, A.M. Farghaly, M.A. El-Semary, A.A. Bekhit, M.S. El-Shoukrofy, Synthesis of some novel pharmacologically active thieno[2,3-d]pyrimidinone derivatives, Alex. J. Pharm. Sci. 25 (2011) 7–14.

[26] H.A. Abd El Razik, M.H. Badr, A.H. Atta, S.M. Mouneir, M.M. Abu-Serie, Benzodioxole–pyrazole hybrids as anti-inflammatory and analgesic agents with COX-1,2/5-LOX inhibition and antioxidant potential, Arch. Pharm. Chem. Life Sci. 350 (2017) e1700026, https://doi.org/10.1002/ardp.201700026.

[27] H.A. Abd El Razik, M. Mroueh, W.H. Faour, W.N. Shebaby, C.F. Daher, H.M.A. Ashour, H.M. Ragab, Synthesis of new pyrazolo[3,4-d]pyrimidine derivatives and evaluation of their anti-inflammatory and anticancer activities, Chem. Biol. Drug Des. 90 (2017) 83–96, https://doi.org/10.1111/cbdd.12929.

[28] R.D. Shah, Phase transfer catalysis assisted Thorpe reaction for the synthesis of 3-aminothiophene-2-carboxylates, E-J. Chem. 8 (2011) 368–372, https://doi.org/10.1155/2011/650501.

[29] V. Lisowski, S. Léonce, L. Kraus-Berthier, J. Sopková-de Oliveira Santos, A. Pierré, G. Atassi, D.-H. Caignard, P. Renard, S. Rault, Design, synthesis, and evaluation of novel thienopyrrolizinones as antitubulin agents, J. Med. Chem. 47 (6) (2004) 1448–1464, https://doi.org/10.1021/jm030961z.

[30] H.M.A. Ashour, I.M. El-Ashmawy, A.E. Bayad, Synthesis and pharmacological evaluation of new pyrazolylbenzenesulfonamides linked to polysubstituted pyrazoles and thiazolidinones as anti-inflammatory and analgesic agents, Monatsh. Chem. 147 (2016) 605–618, https://doi.org/10.1007/s00706-015-1549-x.

[31] H. Zhang, M.S. Bednarz, N.-K. Lim, G. Hernandez, W. Wu, One-pot synthesis of 4-substituted 3-amino-2-cyanothiophenes involving *O*-ethyl thioformate, Org. Lett. 16 (2014) 2522–2525, https://doi.org/10.1021/ol500895t.

[32] S. Pédeboscq, D. Gravier, F. Casadebaig, G. Hou, A. Gissot, F. De Giorgi, F. Ichas, J. Cambar, J.-P. Pometan, Synthesis and study of antiproliferative activity of novel thienopyrimidines on glioblastoma cells, Eur. J. Med. Chem. 45 (2010) 2473–2479, https://doi.org/10.1016/j.ejmech.2010.02.032.

[33] R.J. Kulmacz, W.E.M. Lands, Requirements for hydroperoxide by the cyclooxygenase and peroxidase activities of prostaglandin H synthase, Prostaglandins 25 (1983) 531–540, https://doi.org/10.1016/0090-6980(83)90025-4.

[34] S.A.F. Rostom, I.M. El-Ashmawy, H.A. Abd El Razik, M.H. Badr, H.M.A. Ashour, Design and synthesis of some thiazolyl and thiadiazolyl derivatives of antipyrine as potential non-acidic anti-inflammatory, analgesic and antimicrobial agents, Bioorg. Med. Chem. 17 (2009) 882–895, https://doi.org/10.1016/j.bmc.2008.11.035.

[35] H. Hosseinzadeh, H.M. Younesi, Antinociceptive and anti-inflammatory effects of Crocus sativus L. stigma and petal extracts in mice, BMC Pharmacol. 2 (2002) 7.

[36] G. Daidone, B. Maggio, D. Raffa, S. Plescia, M. Bajardi, A. Caruso, V.M.C. Cutuli, M. Amico-Roxas, Synthesis and pharmacological study of ethyl 1-methyl-5-[2-substituted-4-oxo-3(4*H*)-quinazolinyl]-1*H*-pyrazole-4-acetates, Eur. J. Med. Chem. 29 (1994) 707–711, https://doi.org/10.1016/0223-5234(94)90033-7.

[37] M. Verma, M. Tripathi, A. Saxena, K. Shanker, Anti-inflammatory activity of novel indole derivatives, Eur. J. Med. Chem. 29 (1994) 941–946, https://doi.org/10.1016/0223-5234(94)90193-7.

[38] Molecular Operating Environment 2014.09 (MOE), Chemical Computing Group Inc., Montreal, Quebec, Canada. http://www.chemcomp.com (accessed on 2 November 2018).

[39] J.L. Wang, D. Limburg, M.J. Graneto, J. Springer, J.R.B. Hamper, S. Liao, J.L. Pawlitz, R.G. Kurumbail, T. Maziasz, J.J. Talley, J.R. Kiefer, J. Carter, The novel benzopyran class of selective cyclooxygenase-2 inhibitors. Part 2: The second clinical candidate having a shorter and favorable human half-life, Bioorg. Med. Chem. Lett. 20 (2010) 7159–7163, https://doi.org/10.1016/j.bmcl.2010.07.054.

[40] Y. Zhang, X. Zhang, L. Qiao, Z. Ding, X. Hang, B. Qin, J. Song, J. Huang, Synthesis, structures, drug-likeness, *in vitro* evaluation and *in silico* docking on novel N-benzoyl-N′-phenyl thiourea derivatives, J. Mol. Struct. 1176 (2019) 335–345, https://doi.org/10.1016/j.molstruc.2018.08.069.

[41] Molinspiration. www.molinspiration.com/cgi-bin/properties (accessed on 13 October 2018).

[42] C.A. Lipinski, F. Lombardo, B.W. Dominy, P.J. Feeney, Experimental and computational approaches to estimate solubility and permeability in drug discovery and development settings, Adv. Drug Deliv. Rev. 46 (2001) 3–26, https://doi.org/10.1016/S0169-409X(00)00129-0.

[43] P.A. Channar, A. Saeed, D. Shahzad, F.A. Larik, M. Hassan, H. Raza, Q. Abbas, S.-Y. Seo, Extending the scope of amantadine drug by incorporation of phenolic azo Schiff bases as potent selective inhibitors of carbonic anhydrase II, drug-likeness and binding analysis, Chem. Biol. Drug Des. 92 (2018) 1692–1698, https://doi.org/

10.1111/cbdd.13335.
[44] Y.H. Zhao, M.H. Abraham, J. Le, A. Hersey, C.N. Luscombe, G. Beck, B. Sherborne, I. Cooper, Rate-limited steps of human oral absorption and QSAR studies, Pharm. Res. 19 (2002) 1446–1457, https://doi.org/10.1023/A:1020444330011.
[45] Molsoft software http://molsoft.com/mprop/ (accessed on 13 October 2018).
[46] P. Dhamodharan, N. Ponnusamy, R. Odumpatta, S. Lulu, M. Arumugam, Computational investigation of marine bioactive compounds against E6 oncoprotein of Human Papilloma Virus-HPV16, JAPS 8 (2018) 023–032, https://doi.org/10.7324/JAPS.2018.8404 japsonline.com/admin/php/uploads/2596_pdf.pdf.
[47] Preadmet. preadmet.bmdrc.kr/adme/ (accessed on 13 October 2018).
[48] D.E. Clark, S.D. Pickett, Computational methods for the prediction of drug-likeness, Drug Discov. Today 5 (2000) 49–58, https://doi.org/10.1016/S1359-6446(99)01451-8.